Size Adjustable Separation of Biologically Active Molecules

by

Mauricio R. Gutierrez

Bachelor of Science in Mechanical Engineering, Saint Louis University (2001)

Submitted to the Department of Mechanical Engineering
in partial fulfillment of the requirements for the degree of

Master of Science in Mechanical Engineering

at the

MASSACHUSETTS INSTITUTE OF TECHNOLOGY

June 2004

Author .....
Department of Mechanical Engineering
May, 7 2004

Certified by .....
Kamal Youcef-Toumi
Professor of Mechanical Engineering
Thesis Supervisor

BARKER

Accepted by .....
Ain Sonin
Chairman, Department Committee on Graduate Students

Size Adjustable Separation of Biologically Active Molecules

by

Mauricio R. Gutierrez

Submitted to the Department of Mechanical Engineering
on May, 7 2004, in partial fulfillment of the
requirements for the degree of
Master of Science in Mechanical Engineering

Abstract

Separation of biologically active molecules(BAM's) is a problem for the pharmaceutical and biotechnology industries. Current technologies addressing this problem require too many techniques, toxic additives, and time to filter desired materials. As a result, a new technology is needed. The objective of this thesis is to contribute towards the development of a new method for separating biologically active molecules in the size range of 0.5 nanometers to 500 nanometers. A normally open diaphragm valve is proposed that can control a gap formed by two flat surfaces. For accurate control of gap height, the valve was designed to ensure that the flat surfaces remain parallel during operation . Modularity was also part of design considerations to address issues of eventual biocompatibility breakdown – specifically protein adsorption. Control of the gap has been achieved to increments of 1.8 nanometers.

Thesis Supervisor: Kamal Youcef-Toumi
Title: Professor of Mechanical Engineering

Acknowledgments

Thank my Professor Kamal Youcef-Toumi for his guidance and encouragement to make this project the best it could be. The lessons learned through his advising style have already become apparent. Thank you to the Pablo Valdivia, Dan Burns, Heejin Choi, Osamah El Rifai, Khalid El Rifai, Belal Helal, Namik Yilmaz Ahmed Elmouelhi of the Mechatronics Research Laboratory for their insights helping me to understand concepts needed to complete this thesis. A special thank you to Vijay Shilpiekandula who designed the control system for the closed loop experiments. Thank you also to Mr. Fred Cote of the Edgerton Center Machine Shop for his help manufacturing the parts for this project.

Thank you also to the rest of the MIT community for providing an environment that taught me lessons I will take with me for the rest of my life. I would especially like to thank Mrs. Leslie Regan for her all her help in finding a place in this community and for helping to learn how to adjust to learning to think at MIT. Thank you also to Ed Ballo, Ray Harding, Pierce Hayward, Nick Powley, Chris Guerra, Adam Nolte, Fred Latour, Charlene Ellsworth, and Juhyun Park.

I would also like to thank the community at Saint Ann University Parish and the Tec Catholic Community at MIT for helping me to stay spiritually alive. Special thanks to Fr. John Uni, Letitia Howland, Joe Mazzone, Tim Lannen, Michelle Buckliss, and Liane Marquis. Thank you also to my friends from St. Louis, Matt Moeller, Vickie Weber, Clark Bitney, Bob Purcell, Katy Schluge, April Weiss, Katie Burke, Emily Mason, and Jeff Janson.

There were many people who helped and encouraged me during my time at MIT. I can't name you all, but please know that I do and will remember what you did no matter how insignificant it might seem to you.

Thank you Mr.Ken Taylor and Mrs. Claire Taylor.

To my mom Carmen Cruz-Mendez, Mr. Gerard Greco, and Mrs. Kathleen Greco. Your support and endless encouragement has made this possible. My goals since high school would never have been reached without everything you have sacrificed for me and taught me. I love you. Thank you.

Take Lord and receive

all my liberty, my memory, my understading, and all my will

All that I have and possess.

You, Lord, have given all that to me.

I now give it back to you, O Lord

All of it is yours

Dispose of it according to your will

Give me your love and your grace, for that is enough for me.

–From the Spiritual Excercises of Saint Ignatius Loyola

Contents

1 Introduction – The Problem **18**

1.1 Chapter Summary 18

1.2 Motivation 18

1.3 Design Specifications 19

1.3.1 Material Requirements 21

1.3.2 Temperature Requirements 21

1.3.3 Limited or No Additives 21

1.3.4 Size Range Requirements 21

1.3.5 Flow Rate Requirements 22

1.4 Problem Approach 22

1.5 Document Outline 23

2 Separation Technology Description and Status **24**

2.1 Introduction 24

2.2 Electrophoresis - Separation by Charge and Size 24

2.2.1 Gel Electrophoresis 26

2.2.2 Capillary Electrophoresis 26

2.2.3 Electrophoretic Disadvantages 26

2.3 Chromatography - Separation by Absorbency 27

2.3.1 Chromatography Disadvantages 27

2.4 Membrane Technologies - Separation by Size 27

2.4.1 Membrane Disadvantages 29

2.5 Lab-on-Chip Devices - Advances in Electrophoresis and Chromatography . 30
2.6 The Nanopore - Advancement in Membrane Technology 30
2.7 Valve Based Separations - Advancement in Size Based Separation 32
2.7.1 The Nanogate - Diaphragm Valve 32
2.7.2 The JPL Valve - Diaphragm Valve 32
2.7.3 Tubular Filtration Valve 33
2.8 Conclusion – Separate by Size 33
2.9 Chapter Summary 36

3 Technical Challenges to Valve Based Separation 37
3.1 Introduction 37
3.2 Problem 1 – Creating a 0.5 nm Gap 38
3.2.1 Area of Contact 38
3.2.2 Surface Profile Terminology 38
3.2.3 Roughness 38
3.2.4 Waviness 41
3.2.5 Flatness 41
3.2.6 Profile Measurement 42
3.2.7 Surface Profile Manufacturing 42
3.3 Problem 2 – A Dynamic Gap 47
3.3.1 Structural Requirements 47
3.3.2 Thermal Requirements 47
3.3.3 Actuation Requirements 48
3.3.4 Feedback Requirements 50
3.4 Problem 3 – Fluid Dynamics 52
3.4.1 Surface Tension 52
3.4.2 Fluid Flow 52
3.5 Problem 4 – Biological Compatibility 55
3.6 Problem 5 – A Cost Effective Design 55
3.7 Comparison of Valve Designs 56
3.7.1 The Nanogate Design 56

3.7.2 The JPL Design . . . 56
3.7.3 The Tubular Valve Design . . . 57
3.8 Chapter Summary . . . 57

4 Proposed Design Solution **58**
4.1 Introduction . . . 58
4.2 Design Overview . . . 58
4.3 Prototype Material Selection . . . 59
4.3.1 Structural Materials . . . 59
4.3.2 Flat Plates . . . 62
4.3.3 Coating . . . 62
4.4 Base Design . . . 62
4.5 Midsection Design . . . 62
4.5.1 Physics of a Diaphragm . . . 64
4.5.2 Physics of the Pivot . . . 66
4.5.3 Machining Considerations . . . 69
4.6 Top Housing . . . 69
4.7 Assembly of Base and Top Housing . . . 70
4.8 Actuation and Sensing . . . 70
4.8.1 Initial Sensing System . . . 71
4.8.2 Gap Height Sensing . . . 72
4.8.3 Piezoelectric Actuator Technical Specifications . . . 72
4.8.4 Capacitive Sensor Technical Specifications . . . 73
4.9 Fluid Control . . . 73
4.9.1 Pumps . . . 74
4.9.2 Tubing . . . 74
4.10 Chapter Summary . . . 74

5 Simulations, Experiments and Results **75**
5.1 Introduction . . . 75
5.2 Diaphragm Design Simulations and Experiments . . . 75

5.2.1 Diaphragm Finite Element Analysis – Deflections and Stresses . . . 75
5.2.2 Diaphragm Stiffness Verification–Experiment Number 1 78
5.3 Diaphragm Experiments - Open Loop and Closed Loop Characterization . . 81
5.3.1 Open Loop Motion – Experiment Number 2 81
5.3.2 Closed Loop Characterization of the Diaphragm – Experiment Number 3 81
5.4 The Tilting Mechanism 83
5.4.1 Flexure Finite Element Analysis – Deflections and Stresses 83
5.4.2 Visual Verification of Tilting Concept – Experiment Number 4 . . . 83
5.5 Chapter Summary 83

6 Conclusions and Recommendations **90**
6.1 Short Term Recommendations 90
6.2 Long Term Recommendations 91
6.3 Conclusion 91

A Disregarded Design Ideas **97**
A.1 Appendix A Summary 97
A.2 Design 1 – Tubular Filtration 97
A.2.1 Material Selection 97
A.2.2 Manufacturing Process 98
A.2.3 Design Commentary 98
A.2.4 Design 1 – Bottom Line 99
A.3 Design 2 - Sliding Substrates 102
A.3.1 Overall Design Description 102
A.3.2 Material Selection 102
A.3.3 Manufacturing 102
A.3.4 Design Commentary 103
A.3.5 Design 2 – Bottom Line 103
A.4 Design 3 – Flexure Based Design 104
A.4.1 Overall Design Description 104

A.4.2 Material Selection 105
A.4.3 Manufacturing 105
A.4.4 Design Commentary 105
A.4.5 Design 3 – Bottom Line 105
A.5 Considered Pivot Designs 106

B Calibration of The Capacitance Probes **107**

C Specification Sheets of Purchased and Used Equipment **109**

D Drawings and Pictures of the Machine **115**

List of Figures

1-1 Filtration Spectrum 20
1-2 The Concept 22

2-1 Chromatography Schematic 28
2-2 Membrane Filtration 29
2-3 The Nanopore 31
2-4 The Nanogate 33
2-5 Jet Propulsion Laboratory Microvalve 34
2-6 Tubular Filter 35

3-1 Area of Contact Definitions 39
3-2 Surface Profile 40
3-3 Roughness Peaks and Valleys 40
3-4 Surface Profile Measurement Methods 43
3-5 Metrology Spectrum 44
3-6 Tilt Effects 48
3-7 Actuator Selection Chart 49
3-8 Piezoelectric Actuator Design Types 51
3-9 Surface Tension 53
3-10 Poiseuille Flow 54

4-1 Modified JPL Valve 59
4-2 Base – Prototype 63
4-3 Midsection – Prototype 63

4-4 Diaphragm Model 65
4-5 Flexure Options 67
4-6 Hinge Dimensions and Forces 68
4-7 Top Housing – Prototype 69
4-8 Kelvin Clamp Kinematic Coupling 70
4-9 Graphical Representations For Sensing Closure of the Gap 71
4-10 Block Diagram of Sensing with Capacitive Sensor 72
4-11 How the Probe Measures Displacement 73

5-1 Diaphragm (Aluminum 7075) Displacement Study 76
5-2 Diaphragm (Aluminum 7075) Stress Study 77
5-3 Linear Fit of Diaphragm Applied Force vs. Deflection Experiment 79
5-4 Picture of Diaphragm Motion Control Test 80
5-5 Hysteresis Plot of an Open Loop Controlled Design 82
5-6 Closed Loop Input Actuation Pulse 84
5-7 Closed Loop Output Actuation Pulse 85
5-8 Pivot (Aluminum 7075) Displacement Study 86
5-9 Pivot (Aluminum 7075) Stress Study 87
5-10 Demonstration of Tilt Compensation Flexure 88

A-1 Displacement With Applied Force 99
A-2 Tubular Filtration - Gap Drawing 100
A-3 Tubular Filtration - Molded Tube Version 101
A-4 Substrate Sliding 102
A-5 Flexure Idea 1 104
A-6 Close-up cross-section of diaphragm with pivot 106

B-1 Capacitance Probe Calibration Check 108

C-1 Specifications for Used Capacitance Probes 110
C-2 Specifications for Piezoelectric Amplifier used in Chapter 5 experiments . . 111
C-3 Piezoelectric used in Chapter 5 experiments 112

C-4 Piezoelectric Actuator specified in Chapter 4 113
C-5 Piezoelectric Actuator specified in Chapter 4 114

D-1 Base Specs 116
D-2 Diaphragm Specs 117
D-3 Built Diaphragm Pictures 118

List of Tables

2.1 Summary of Reviewed Contemporary Technologies 25

3.1 Roughness Manufacturing Methods 45

4.1 Selected Material Properties 61

Chapter 1

Introduction – The Problem

1.1 Chapter Summary

This chapter introduces the reader to the motivations for this project. User requirements are provided with some explanation for each specification. The basic concept of the design is presented. An outline for the remainder of the document concludes the chapter.

1.2 Motivation

Separation of biologically active molecules (BAMs) is critical to the pharmaceutical and biotechnology industries. The ability to isolate molecules is important because it facilitates activities like:

- Determining the structure of the molecule,
- identifying the active component of a mixture, and
- studying molecule properties without the added constraints of its interaction with complex mixtures [1],

Contemporary separation methods are costly, time consuming, bulky, can be easily contaminated, and do not provide the needed resolution. In addition, some of the chemicals utilized for processing are toxic to humans (See Section 2.2.3 on page 26). As a result, available technologies are inherently inadequate.

This project is part of ongoing research aimed towards the development of a smart ultra-mechatronic filter for molecule separation and characterization. The specific focus is the development of a separation method that is not limited by the shortfalls of separation methods that are currently used. Molecules to be separated (aqueous salts, proteins, DNA) span from the Ionic Range to the Macro-Molecular Range (See Figure 1-1) for the full spectrum). These molecules correspond to a size range of 0.5 nm to 500 nm. The goals for the completed mechatronic device can be summarized by the following commentary:

> The ramifications of such a machine are astounding: imagine pharmaceutical companies with hundreds of billions of dollars in R&D and thousands of acres of laboratory space, dedicated to purification of compounds, shrinking down to desktop-size smart mechanotronic filters, which are capable of fishing out new therapeutic candidates from Amazon forest within few hours rather than years of hard work; imagine every household with the most sophisticated lab to identify pathogens, analyze blood, urine and every other body fluid and much more within 15-30 seconds. [34].

1.3 Design Specifications

From the user standpoint, in order for the technology to be viable and competitive the following requirements are to be met:

1. All materials interfacing with the sample to be separated must be chemically and biologically inert, and minimize adhesion,
2. The technology should keep the sample at a desirable operating temperature,
3. Limited or no additional chemicals should be added to enhance separation,
4. The technology should be capable of distinguishing between molecules with size differences as small as 1 angstrom [34], and
5. The flow rate of the separated molecules in the device should be between 10 - 20 μL/min at minimum [34],

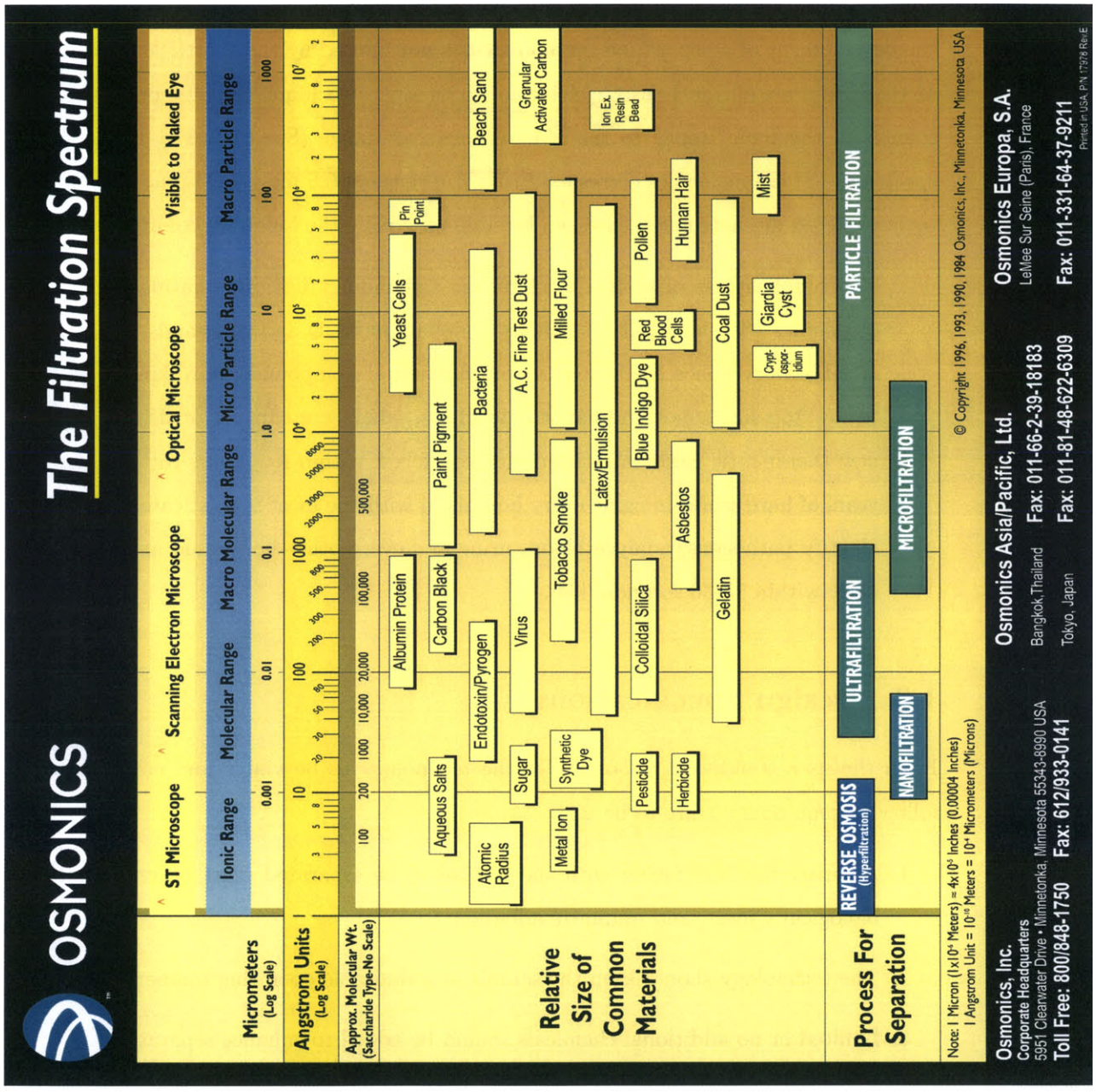

Figure 1-1: Filtration Spectrum
Courtesy of General Electric Water Technologies [12]

1.3.1 Material Requirements

Chemical and biological inertness is essential to any machine dealing with BAMs. Non-inert materials release chemicals which react and could alter the physico-chemical characteristics of the sample to be separated [44]. Minimal or no adhesion of the sample to the filtering materials is also desirable to prevent biofouling and cross-contamination when a new sample is inserted into the device. At this time, no materials fulfill the adhesion requirement. Materials that do not release agents harmful to BAMS are available.

1.3.2 Temperature Requirements

Biological molecules are sensitive to environmental changes. DNA for example, can denature if the temperature is too hot. In order for this technology to be non-destructive to a wide variety or molecules, it must be capable of handling samples at temperatures of 4^0C. Heat addition to the sample should be minimized.

1.3.3 Limited or No Additives

During the process of investigation, a sample cell is typically ruptured and its contents homogenized. The contents are mixed with additives that enhance separation and/or allow for the detection of small molecules. Recovery steps are required to separate sample molecules from the additives. This leads to increased separation time and sample loss. For this reason, it is desired that few additives be used.

1.3.4 Size Range Requirements

Molecule sizes and shapes depend on the strength of the bonds between elements, and the number of elements present. Exact dimensions of individual atoms are difficult to obtain. It is unknown what the minimal change in dimension between two molecules could be. Angstrom resolution was chosen because it is the limit of what has been shown to be possible with available technology [47][21].

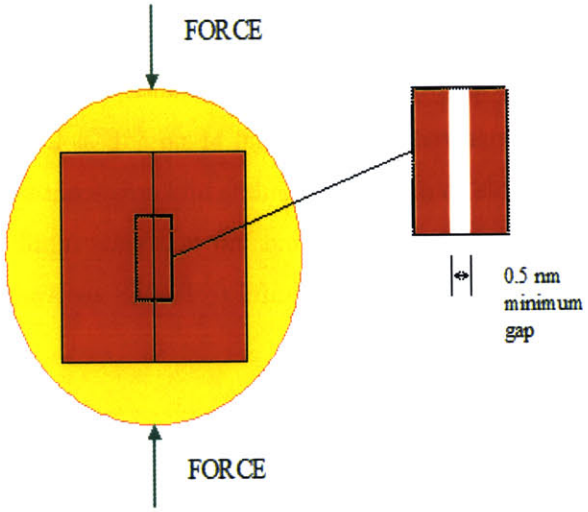

Figure 1-2: The Concept
Create a gap and control the distance between its two boundaries.

1.3.5 Flow Rate Requirements

One of the user goals is to provide separation in a short amount of time. A precise separation technology with minimal flow rate of 10 μL/min for the smallest gap would be competitive and useful to the market.

1.4 Problem Approach

Different physico-chemical properties (for example size, shape, electrical charge, acoustic radiation, etc.) can be used to achieve separation. This project's goal is to make contributions towards achieving the ultra mechatronic device by expanding and improving on a concept for a mechanically programmable filter that separates molecules by size.

The concept is simple: create a gap and control its smallest dimension [37] [14]. The most recent version of this device created a gap by placing two flat plates together. Gap size selection was achieved by actuating a flexible material that surrounded the flat plates(See Figure 1-2) [37].

1.5 Document Outline

The rest of this document will be organized as follows. Chapter 2 will discuss the possible technological approaches towards separation of biological molecules. A case will be made for the selection of separation by size. Chapter 3 will discuss some of the technical challenges facing any device that will dynamically separate BAMs by size. Chapter 4 will present a design aimed at achieving the goals presented in this and following chapters. Chapter 5 will present simulations, experiments and results aimed at demonstrating the validity of the proposed design. Chapter 6 concludes the document and presents the basis for future work.

Chapter 2

Separation Technology Description and Status

2.1 Introduction

This chapter will review technologies utilized to separate biological molecules. Proven technologies include: electrophoresis, chromatography, and membrane. Electrophoresis separation is mainly a charge based separation . Chromatography separates through differentiation in absorbency. Membranes separate by size differentiation. Technologies on the horizon include lab-on-chip devices, the Nanopore, and the valve based approach. Lab-on-chip devices miniaturize electrophoretic and chromatographic techniques. The Nanopore is a membrane based development. Valve based designs utilize a controllable gap to separate by size. Based on a comparison of these technologies, valve based separation is the best fit towards achieving the user requirements.

2.2 Electrophoresis - Separation by Charge and Size

Electrophoresis is the term given to technologies that separate molecules according to the distance they travel under the influence of an electric field. Two popular electrophoretic methods are gel electrophoresis and capillary electrophoresis.

Technology Category	Process	Separation Property	Advantages	Disadvantages
Electrophoresis	Gel Electrophoresis	Charge and Size	• Resolution	• Process Time • Safety
	Capillary Electrophoresis	Charge and Size	• Resolution • Process Time	• Difficulty in separating neutrally charged molecules
Chromatography	Gas Chromatography	Solubility	• Resolution	• Separation Range Requires Validation • Hazardous Chemicals • Limited to Volatile Chemicals
	HPL Chromatography	Solubility	• Resolution	• Separation Range • Requires Validation • Uses Hazardous Chemicals
Membrane	Nanofiltration	Size	• Resolution • Buffer Free	• Set to 1 specific size • Biofouling • Requires multiple passes
	Ultrafiltration	Size	• Resolution • Buffer Free	• Set to 1 specific size • Biofouling • Requires multiple passes
	Microfiltration	Size	• Resolution • Buffer Free	• Set to 1 specific size • Biofouling • Requires multiple passes

Table 2.1: Summary of Reviewed Contemporary Technologies
This chart provides a summary of the advantages and disadvantages of technologies discussed in this chapter. Each technology is broken down by broad categorization followed by a specific process. The characteristic used to achieve separation is identified along with advantages and disadvantages.

2.2.1 Gel Electrophoresis

In gel electrophoresis, a biological sample is mixed with a buffer and inserted into a gel. The rate of molecule movement is dependent on size and charge. Gels are polymers (usually agarose or polyacrylamide) that form a porous medium when polymerized. Size of the pores is determined by the amount of cross-linker and the amount of polymer in the gel [19]. When an electrical field is applied, the molecules are forced to move through pores in the gel. Cations move toward the cathode and anions move toward the anode. In addition to the charge separation, the pores in the gel hinder the movement of larger molecules. After a given amount of time the electric field is turned off and molecules of different size and charge are located in different regions of the gel [39].

2.2.2 Capillary Electrophoresis

Capillary electrophoresis is similar to gel electrophoresis with the exception that separation takes place in a capillary. The capillaries generally range in length from 30 to 50 cm. Outer diameters range from 0.150 mm to 0.375 mm. Inner diameters range from 0.010 mm to 0.075 mm [42]. The capillary is filled with a buffer and a sample. An electric field is then applied and the sample separates according to charge. Capillary electrophoresis has high separation efficiency, requires a small sample, and separates very quickly (1 to 45 minutes) [31].

2.2.3 Electrophoretic Disadvantages

Despite advancement of electrophoretic techniques, both gel electrophoresis and capillary electrophoresis fall short of the requirements for this project. For both methods, the procedure is not always uniform. Gels of different pore dimensions must be made. Capillary electrophoresis requires different techniques for separating molecules with properties varying to the degree required for this project (See 1.2). Gel electrophoresis has the added disadvantage that only low voltages can be applied to avoid overheating and denaturing of the sample. As a result, it is extremely slow.

The number of buffers and added materials for electrophoresis to work can be the cause of work hazards. For example, Ethidium Bromide (used for visualization of DNA) is a

known carcinogen [19]. Acrylamide is also a known nerve toxin [27] and is reported to be clastogenic(causes chromosomal abberations) [26].

2.3 Chromatography - Separation by Absorbency

Chromatography categorizes a broad set of physical separation methods in which the molecules to be separated are distributed between two phases, one is stationary and the other is mobile (See Figure 2-1). A sample to be separated is dissolved in the mobile phase (a gas, liquid or supercritical fluid). The mobile phase and sample mixture is then forced through the stationary phase (typically a column or paper). Different samples have different mobilities in the two phases. The interaction of the dissolved mixture with the two phases affects the travel time of different molecules. As a result, sample components separate when travelling through the stationary phase. The main benefit that Chromatography provides is that it can separate complex mixtures efficiently [11].

2.3.1 Chromatography Disadvantages

The main disadvantage of chromatography is that no one chromatographic method can separate the full range of molecules desired for this project. Gas chromatography, for example, only applies to volatile samples. Ion exchange chromatography typically applies to proteins and organic ions. Gel permeation applies to removing buffer ions from a sample. Another significant disadvantage of chromatography is that it requires validation of homogeneity by some other means (typically electrophoresis).

2.4 Membrane Technologies - Separation by Size

There are three terms which describe the filtration process at the macromolecular range: Hyperfiltration (or Reverse Osmosis), Nanofiltration, Ultrafiltration, and Microfiltration. These processes all work under the same basic concept. A semi-permeable membrane is used to allow the fluid being separated to pass through it. Pore sizes of the membranes differentiate the filtration names (with some overlap). Membranes are typically made of cellulose, Teflon, and nylon polymers [15].

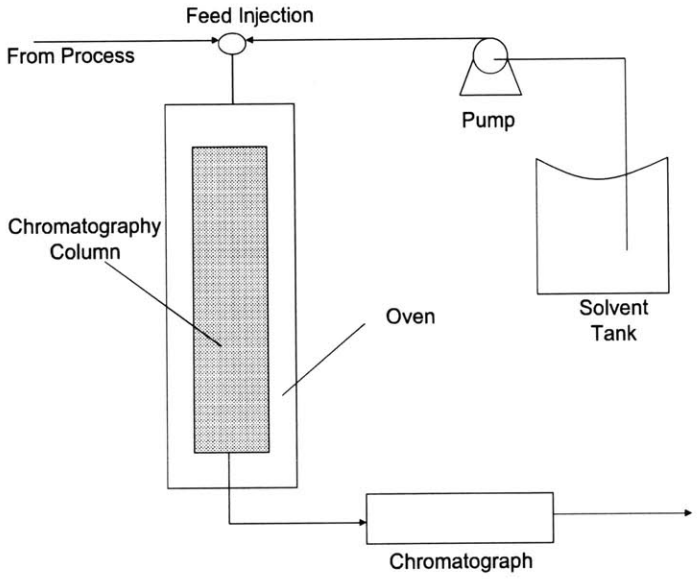

Figure 2-1: Chromatography Schematic
In chromatography, a sample (From Process) and a mobile phase (in Solvent Tank) are mixed and inserted into the stationary phase (in this case the Chromatography Column). The interaction of the mobile phase and sample with the stationary phase determines how the sample is separated. Once separated, the sample is detected using the chromatograph. Courtesy of Kevin Yip [49]

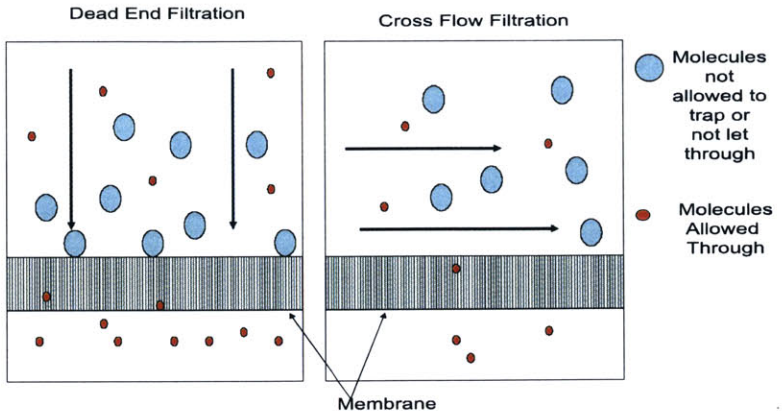

Figure 2-2: Membrane Filtration
In membrane filtration, molecules bigger than the pore sizes are either not allowed through or trapped by the membrane. All other molecules are allowed through. The filtration techniques are differentiated by the direction of the flow.

There are two types of flows cross flow and dead-end. In cross flow filtration, the rejected particles are continuously carried away from the membrane surface. In dead-end filtration, the particles are either trapped in the membrane or build up on top of it (see Figure 2-2). In both cases, the flow is pressure driven.

2.4.1 Membrane Disadvantages

Membrane filtration comes close to the requirements of this project but still falls short. The main disadvantage is fixed pore sizes. The effect of this is that solutions can only be separated by two categories: molecules which are bigger than the pore and molecules that are smaller than the pore. Pore sizes can not be uniformly manufactured throughout the membrane. As a result, some molecules larger than desired can enter the membrane and clog up some passage ways or make it entirely through. Multiple passes through the membrane must be made which results in significant sample loss.

2.5 Lab-on-Chip Devices - Advances in Electrophoresis and Chromatography

The relatively recent advances in MEMS technology have brought with it the idea of miniaturizing the chemical/biological laboratory to the size of a microchip. Electrophoretic and chromatographic methods have been adapted for lab-on-chip devices. Membrane technologies have not been miniaturized in the same way because pore sizes can not be controlled with sufficient accuracy.

In general, these devices are made of Silicon or plastic (PolyDimethylsiloxane in particular). Flow in these devices is driven by pressure and/or electricity.

Miniaturization provides definite improvements on established technological separation concepts. Advantages include the ability to work with smaller samples, potentially faster analysis times, automation, and a lower cost [23]. Although this is desirable, these advances do not offer a fundamentally new method of molecule separation. As a result, the technology fails for the same reasons as non-miniaturized instruments. Buffers are still required and multiple techniques are necessary for isolating a broad variety of molecules.

2.6 The Nanopore - Advancement in Membrane Technology

The Nanopore is either "a protein channel in a lipid bilayer or an extremely small isolated 'hole' in a thin, solid-state membrane" [46]. The idea is that when a molecule passes through the hole (which is not too much bigger than the molecule) it causes changes in the electrical properties of the membrane which can be detected. The Nanopore is at the forefront of research for the membrane based approach to size based separation.

At the time of this writing the Nanopore has only been demonstrated for the detection of DNA (See Figure 2-3). It is unclear whether it will find applications with proteins or other biological molecules. Although the pore size can be altered by heat application, size variation is limited to several nanometers. Size variation is limited both by the amount of heat that can be applied before the sample is degraded and also by the properties of the membrane itself. These limitations make this approach inappropriate for the application of this project.

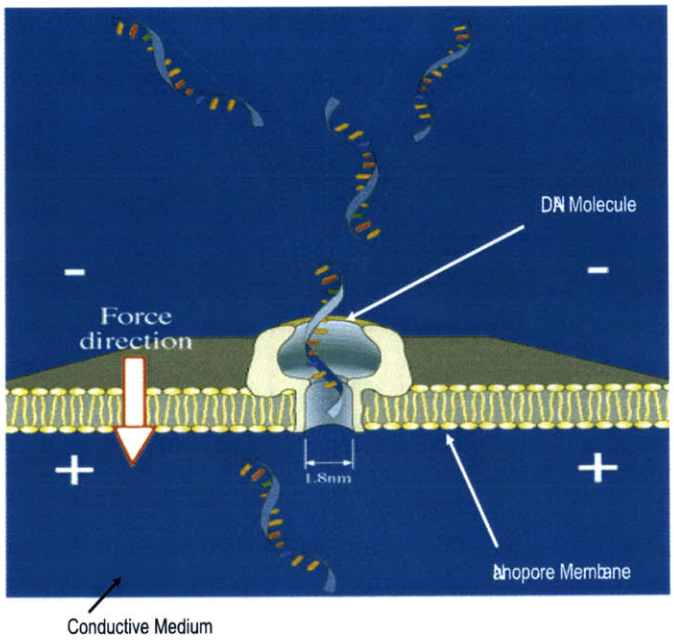

Figure 2-3: The Nanopore
The Nanopore is a protein membrane with a nanometer sized pore. DNA and a conductive fluid surrounds the membrane. Voltage can be measured across the pore due to the flux of conductive fluid. When a DNA molecule passes through the pore, the voltage measurement is altered. This alteration is dependent on the size of the DNA molecule. Courtesy of Sean Ling Group at Brown University [4]

2.7 Valve Based Separations - Advancement in Size Based Separation

An approach of recent interest has been the development of valves for size based separation. These technologies allow for precise control of gap size thus limiting the molecules that can pass through. This advantage can potentially reduce the need for buffers and additives to facilitate separation. In addition, with a properly coated surface there is no sample loss.

The drawback of this approach is that a single working valve can not process a sample quickly. The flow rate is proportional to the gap height cubed. This technology can also be a more costly investment. Molecules will eventually attach to the surfaces. As a result, the separation apparatus must be cleaned or disposed of.

Several examples of this technology follow.

2.7.1 The Nanogate - Diaphragm Valve

The Nanogate is a circular flexure that is manufactured by etching silicon and selectively bonding it to Pyrex glass (see Figure 2-4 for the cross-sectional view). Piezoelectric actuators are then used to deflect the cantilevered plate. Interferometric methods are used for sensing of the gap size. At this time, it has demonstrated controlled gas flows as small as 2 angstroms and liquid flows as small as 70 nm. [47]

2.7.2 The JPL Valve - Diaphragm Valve

This valve was designed by researchers at the NASA Jet Propulsion Laboratory. Although the valve was designed for a space travel applications, its design is worth examining. The design is normally-closed and consists of three core parts: the base (or seat), the diaphragm, and the actuator (see Figure 2-5). The base contains the inlet, outlet and 20μm high rings. The purpose of the valleys between the rings is to trap small particles when closing the gap. A piezoelectric actuator is placed on top of the diaphragm and contracts when a voltage is applied. The three parts are assembled by a heating and pressing process that forms a metal-to-metal diffusion bond. Diaphragm and seat dimensions are 16 mm x 16 mm x 0.4 mm [8].

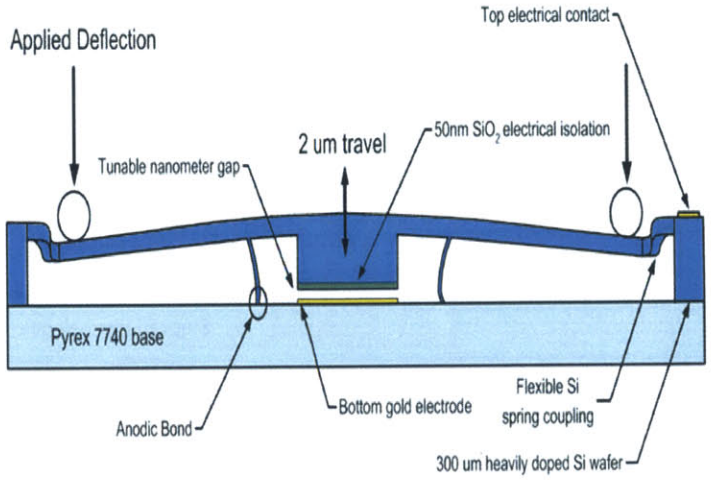

Figure 2-4: The Nanogate
Courtesy Responsive Environments Group – MIT Media Lab[24]

2.7.3 Tubular Filtration Valve

In this design, a fluid flowing inside a silicone and polypropylene tube is filtered when it encounters an obstruction ('the filtering element'). The components of the filtering element include two flat plates (held inside Aluminum holders) placed in close contact and a surrounding flexible element (see Figure 2-6). The metal holders extend outside of the tubing to provide an area for displacement sensing [37]. Sensing is provided by capacitive sensors.

2.8 Conclusion – Separate by Size

In comparing the methods described in this section, it seems that separation by size through a valve design is the logical method to explore because it meets most of the requirements. It is the least harmful method of separation because it does not generate heat, can theoretically be done without the use of buffers, and is adjustable to address size range requirements. For a single gap the flow rate can not be met. If many passageways are available, the flow rate should not be an issue. Detailed challenges will be discussed in the next chapter.

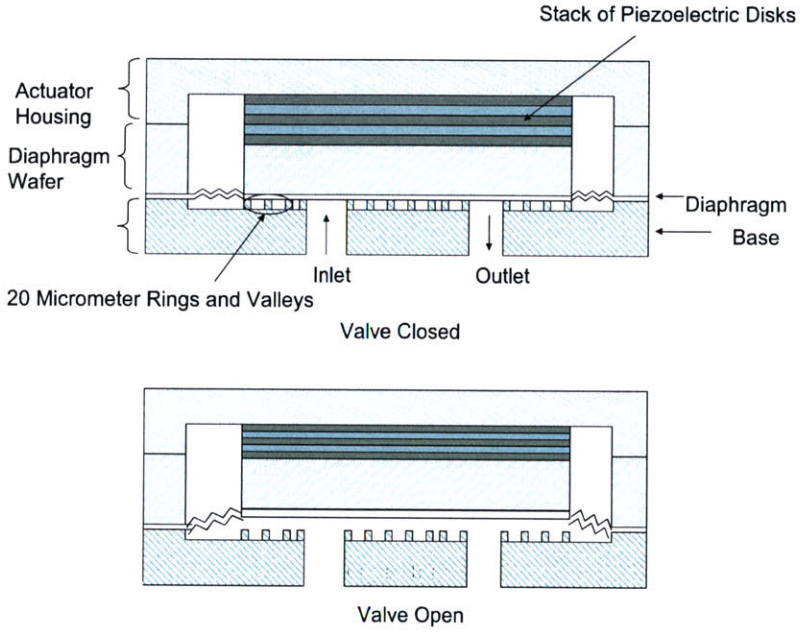

Figure 2-5: Jet Propulsion Laboratory Microvalve
Courtesy of NASA Jet Propulsion Laboratory [8]

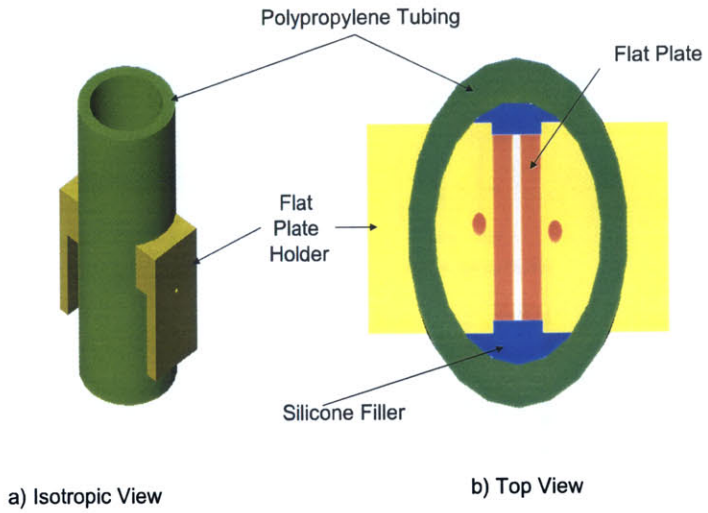

Figure 2-6: Tubular Filter

2.9 Chapter Summary

This chapter reviewed and compared contemporary technologies and technologies in development for the separation of biologically active molecules. Based on this review it was determined that separation by size is the logical approach for this research project.

Chapter 3

Technical Challenges to Valve Based Separation

3.1 Introduction

The previous chapter focused on different approaches towards the separation of molecules. It stated the reasons for undertaking a size based separation approach. This chapter will refine the user requirements with a technical emphasis for a valve based approach. The challenges can be categorized as follows:

1. creating an adjustable gap with an initial opening of 0.5 nm,
2. developing a reliable and controllable mechanism for adjusting the gap,
3. obtaining an adequate flow rate (10 - 20 μL/min) through a well contained pathway,
4. ensuring biological and chemical compatibility of surfaces interfacing with the macromolecules, and
5. making the design cost effective through modularization.

The chapter ends with a comparison of the valve designs presented in Chapter 2.

3.2 Problem 1 – Creating a 0.5 nm Gap

Creation of an adjustable gap requires that two perfectly mating surfaces be placed 0.5 nm apart or that two surfaces with high levels of flatness be placed in contact to create the gap. In either case it is important to understand the terminology, processes, and limits related to creating flat surfaces.

3.2.1 Area of Contact

Surfaces usually do not fully meet when they come in contact. There are two areas of contact to think about: the apparent area of contact and the true area of contact. Apparent area of contact is the area defined by the macroscopic boundaries of the workpiece. True area of contact is much smaller than the apparent area of contact. It is dependent on the asperities of the workpiece and the normal force resulting from contact of the two surfaces (See Figure 3-1). Increasing the normal force or minimizing the size of the asperities increases the true area of contact. Normal force increase is limited by the strength of the workpieces. Asperity minimization is limited by material selection and available manufacturing processes.

3.2.2 Surface Profile Terminology

Surface profiles are determined by the spatial frequency in which they lie (See Figure 3-2). In general, the highest frequency or shortest wavelength component of the surface is referred to as the roughness. The medium range frequency or wavelength is referred to as waviness or nanotopography. The term waviness will be used in this thesis. Flatness or form is the lowest range frequency. The term flatness will be used in this thesis. Additional terms to know are lay, which refers to the direction of the surface pattern. Flaws are unintentional interruptions of the topography.

3.2.3 Roughness

Roughness describes the finest irregularities present on a surface. Numerical measurement is typically about a graphical centerline. The centerline is parallel to the general direction of the surface profile and it is defined such that the areas above and below the centerline are

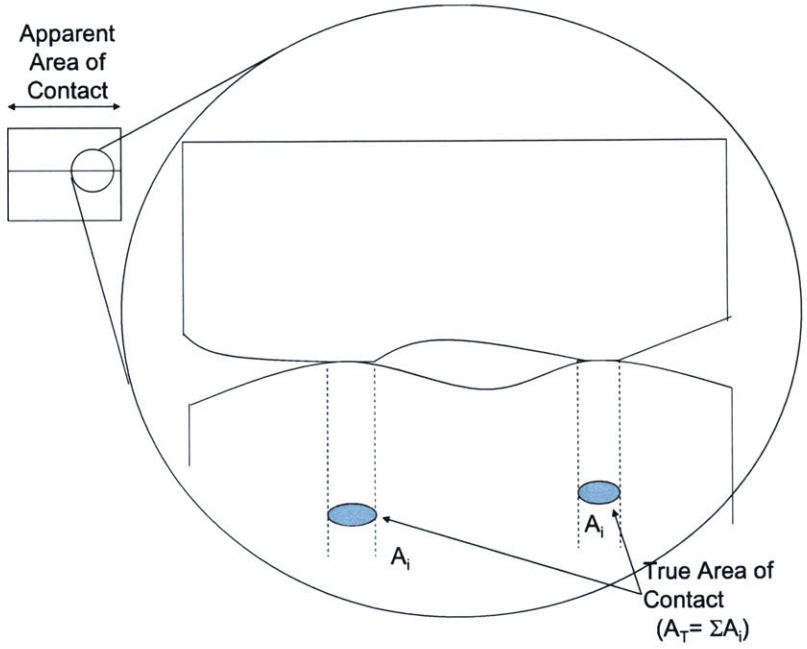

Figure 3-1: Area of Contact Definitions

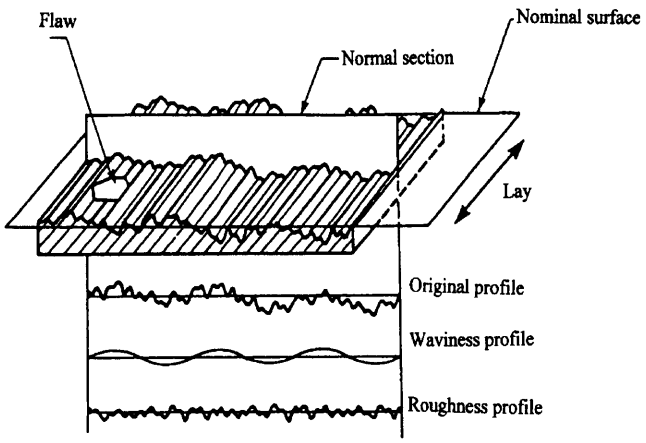

Figure 3-2: Surface Profile
Courtesy of the American Society of Mechanical Engineers [2]

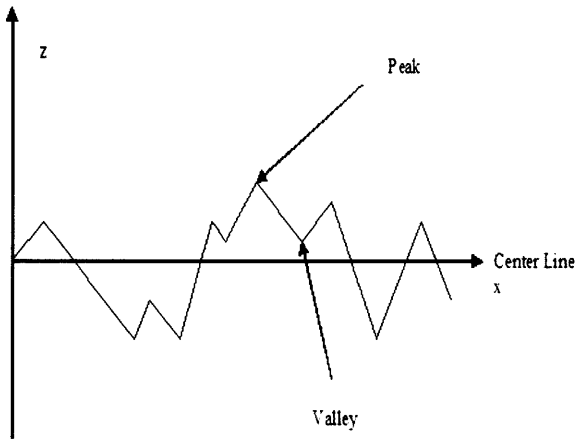

Figure 3-3: Roughness Peaks and Valleys
Roughness is measured about a graphical centerline such that the total area above and below the centerline are equal.

equal. Roughness is typically given a value of Roughness Average (Ra or Rq). This value is the root mean square average of the absolute value of measured height deviations (see Figure 3-3). Peaks are defined to be points of maximum height and valleys are points of maximum depth. The peak to valley height is typically 3 to 4 times the roughness average. Mathematically, Rq is represented by the following equation:

$$Rq = [\frac{1}{L}\int_0^L z^2(x)dx]^{\frac{1}{2}}$$

where 'L' is the length of the surface profile, and 'z' is the deviation of the surface profile from the mean line. Roughness can be caused by the action of the cutting tool or it can be the physical structure of the material.

3.2.4 Waviness

Waviness is more widely spaced component of the surface texture. It is generally the result of machine vibrations, chatter, heat treatment, or warping strains. It is superimposed on the roughness.

3.2.5 Flatness

Flatness refers to the amount of curvature present in a material (the overall shape of the material without regard to roughness and waviness). It is dependent on the thickness and surface area of the material in question. It can be caused by a combination of factors ranging from the part being held a particular way to the stresses in the material. Flatness is on a scale much larger than roughness. Usually flatness is determined by the light distortion method.

In essence, one may want to think of the surface profile by the following analogy:

> Imagine being in a desert. The roughness can be considered the deviation between grains of sand. The waviness would be analogous to the sand dunes. The flatness would be analogous to the curvature on the earth. (Adapted from **??**

3.2.6 Profile Measurement

Surface profiles can be measured in several different ways. The most popular methods are: light interference methods and stylus methods (see Figure 3-4).

The profile can be measured by moving a stylus across the surface of the workpiece. Dimensions of the stylus must be chosen appropriately for the desired tolerance of the measurement. Atomic Force Microscopes are an example of the technology used for stylus profiling. As the stylus moves across the sample length of the workpiece, a filter is used to separate the roughness, waviness, and flatness. Please see reference [40]

Measuring by light interference requires the use of an optical flat. An optical flat is a transparent block typically manufactured from fused quartz, silica, or borosilicate glass. The faces of the flat are finished to fine limits. When the surface in question is placed on the flat, deviations between the two surfaces allow for the presence of air gaps. Light rays reflected through the work surface and underside of the workpiece interfere or reinforce each other. This interaction allows for the measurement in profile deviation. Please see reference [3] for more information.

There is no clear separation mark for the spatial frequencies that define roughness, waviness, and flatness. It depends on the application, workpiece in question, and on the limitations of the filter used to separate out the wavelengths. There is some some overlap to the terms. For the purposes of this project the following scale shall be used. Roughness will cover spatial wavelength range of 2 nm to 100 microns. Waviness will cover the spatial wavelength between 100 microns and 20 mm. Flatness will cover the spatial wavelength between 20 mm and 200 mm (See Figure 3-5).

3.2.7 Surface Profile Manufacturing

Surface metrology depends on the material used and process. Table 3.1 shows some of the typical ways of achieving the desired roughness. The chart shows that the most applicable manufacturing methods are lapping and super finishing (also called super polishing) and that the materials to consider are glass/ceramic and silicon substrates. The two industries that use these manufacturing methods are typically the Optics and Integrated Circuit industries. Both lapping and super polishing are used together to achieve the best results.

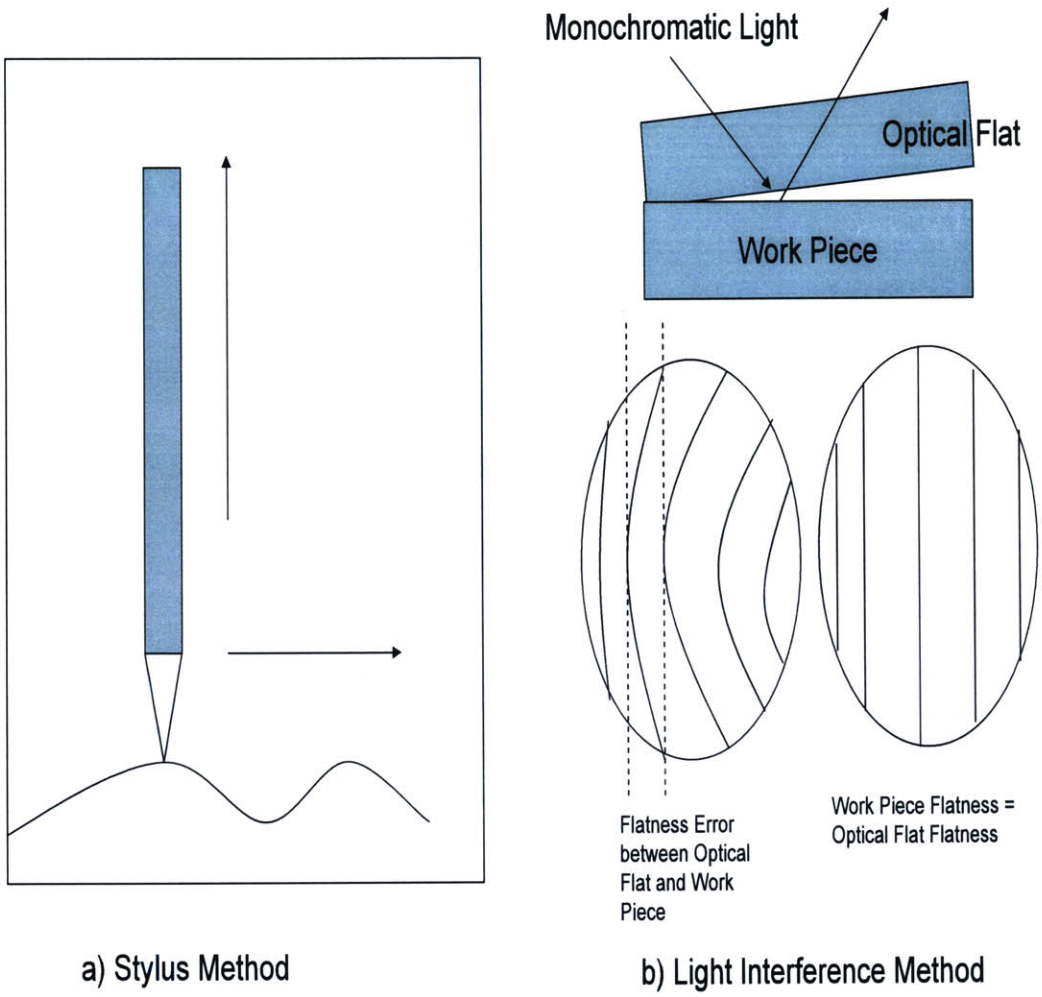

Figure 3-4: Surface Profile Measurement Methods
Part a shows a fine point stylus moved across the surface in question. Part b is adapted from a picture in [28]

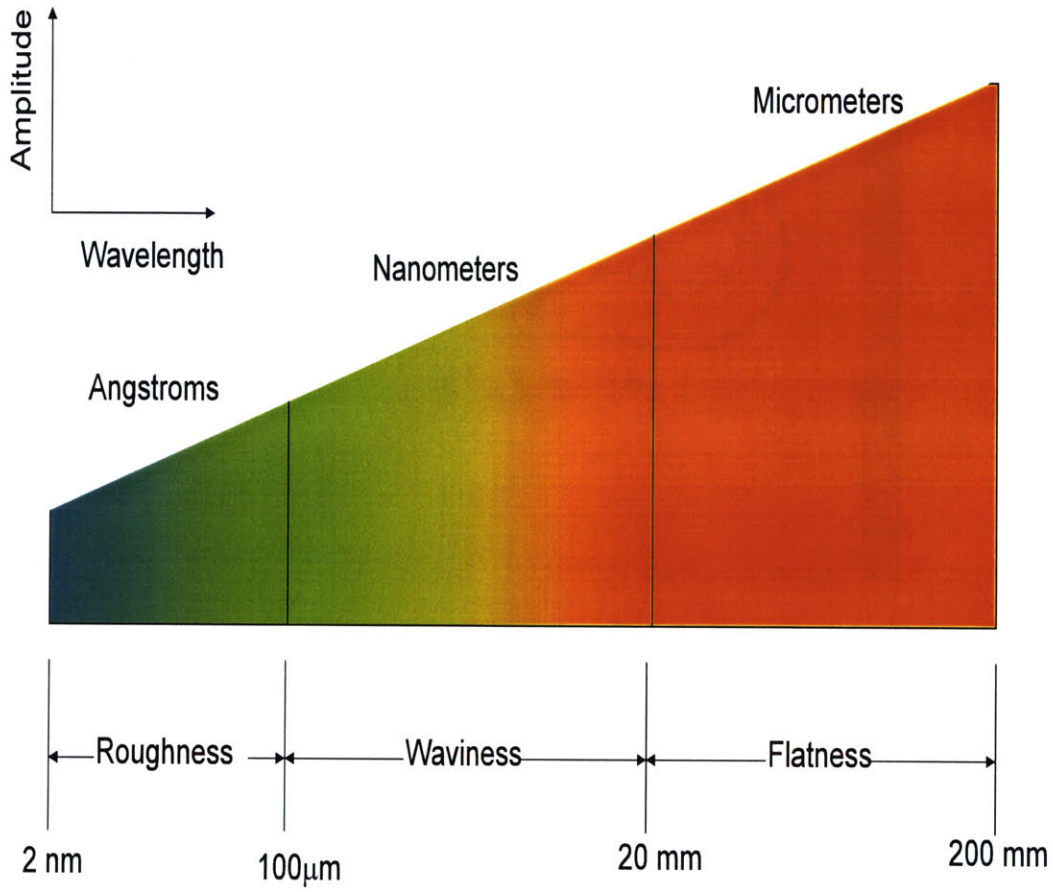

Figure 3-5: Metrology Spectrum
This chart shows typical surface finishes for the given spatial wavelengths. For each given wavelength range, the amplitude is given(Angstrom,Nanometers,Micrometers). Adapted from a Chart Made by Chapman Instruments [45]

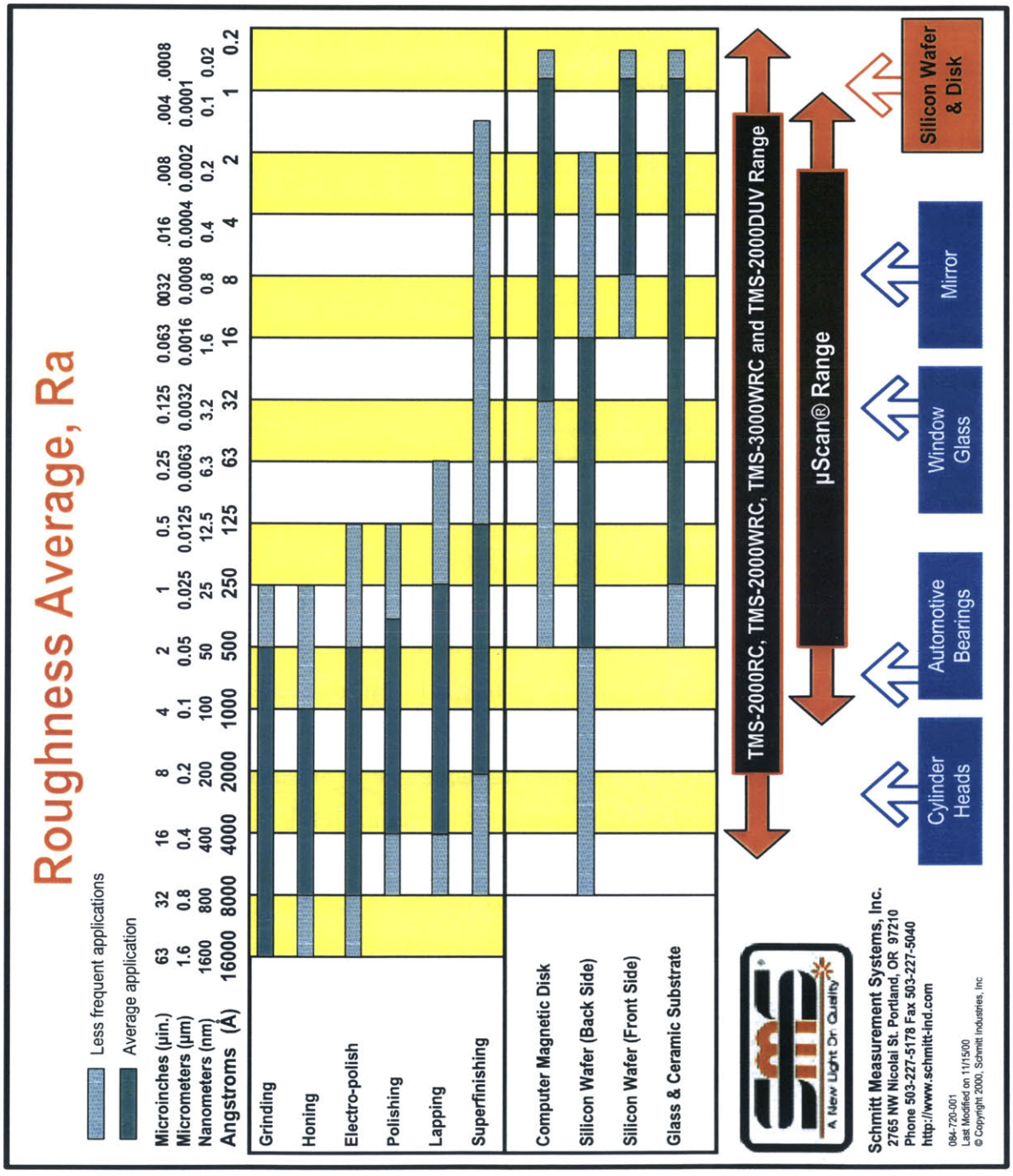

Table 3.1: Roughness Manufacturing Methods
Courtesy of Schmitt Measurement Systems [20]

The idea behind lapping is to place two roughly flat surfaces in contact and rub them together. Both surfaces, as a result, wear down the high spots. In terms of wafer manufacturing it is used to reduce wafer thickness. For the purposes of this project, lapping is the process which affects flatness. Optical fabrication houses typically use diamond impregnated materials in combination with a wet abrasive to loosen the surface peaks [17].

Super polishing can be defined as "the optical process, following grinding, that puts a highly finished, smooth and apparently amorphous surface on a lens or a mirror" [17]. It is a necessary step because lapping leaves the surface of the material scratched and damaged. Polishing produces a smoothing effect across the surface. In general, it is very difficult to achieve surfaces with flatness better than $\lambda/10$ (63.3 nm) because parts tend to spring back once the part is removed from the polishing machine. It is possible to achieve better surfaces but it is also very expensive.

Other methods can also be used to achieve the surface specifications and are being explored for this project. One possible method is to mold a gold monolayer on top of cleaved Mica. Mica is one of the flattest materials when it is separated through this method but can not be used directly because DNA attaches to it. The gold surface can be molded by attaching one side to a Silicon substrate and the other to Mica. Once the gold dries, it can be removed from the mica by bathing it in a chemical liquid. The Gold then produces atomically flat terraces (1 - 2 Angstroms) of approximately 300 nm across. Flame annealing for 30 - 60 seconds can increase the terrace size to approximately 530 nm across. Beyond that range, the deviation is approximately 1 - 2nm. [43]

Another method that could be tested is to compress one part into the other. When two parts come in contact, a percentage of the surface touches due to the surface roughness. The area of contact can be increased by increasing the pressure on one of the parts and thus plastically deforming the peaks on the contacting surfaces. Note that only one surface needs to deform. This results in perfect mating. The downside of this situation is the unknown amount of springback that can result when the two pieces are separated.

In terms of the overall difficulties of this project, the flatness problem is most likely the first that will be solved. Both the IC and Optics industries require materials that are flatter than what is currently available. There is a lot of research focused on improving the surface

profile.

3.3 Problem 2 – A Dynamic Gap

The user desires the ability to increase the initial gap opening of 0.5 nm to at least 500 nm with a resolution of 1 angstrom. An understanding of the structural, thermal, actuation, and sensing limitations is essential for this purpose.

3.3.1 Structural Requirements

Precision control at sub nanometer levels requires smooth, continuous, and wear free motion. Any motion with energy dissipation is difficult to control with sufficient repeatability. As a result, friction, hysteresis, and permanent plastic deformation are to be minimized or avoided in the design.

In order to avoid hysteresis and friction, the motions of the device must depend solely on elastic deformations. Plastic deformation is avoided by not surpassing the yield point of the material in use. Devices that fit this description are called flexures. Flexures are typically constructed out of metals. Range of motion is typically 10 - 15% of the largest dimension. Stiffness of the material is used to hinder undesired motion while compliance is used to promote motion.

In changing the gap size, one must also be sure to avoid lack of parallelism between the two surfaces to be separated (See Figure 3-6). Parallel motion is important because it makes it easier to determine what size gap has been created. In addition, a gap without tilt compensation is thought to create an area where larger particles could enter and either clog the gap or become obstacles to re-closing the gap.

3.3.2 Thermal Requirements

In addition to the structural challenges, any material chosen for this application must be insensitive to thermal fluctuations. Sensitivity to temperature variations can have disastrous effects on the dimensional stability of the design. For this reason, the coefficient of thermal expansion must be considered. Materials like Silicon, Fused Silica, and Zerodur are

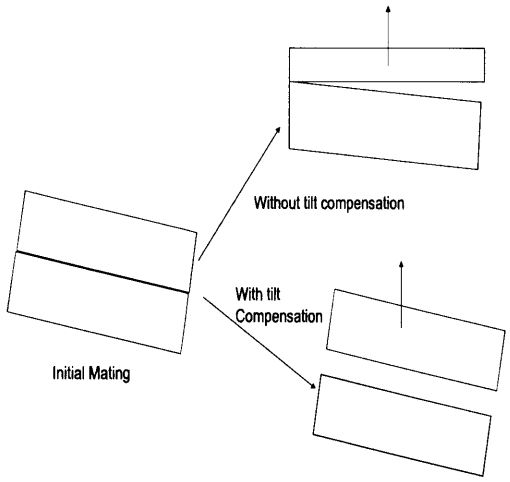

Figure 3-6: Tilt Effects

appropriate to investigate with this regard.

3.3.3 Actuation Requirements

Energy dissipation (i.e. friction/stiction) must also be eliminated in the actuator to achieve nanometer or better resolution. There are essentially three actuation options: voice coil actuators, electromagnetic actuators, and piezoelectric actuators. Piezoelectric actuators are used if there is less than 40 microns of motion, voice coil actuators are used for motion between 40 microns and 100 mm, linear actuators apply between 75 and 100 mm [7] [41] (see Figure 3-7).

Piezoelectric actuators will be used for this project because the gap size need not exceed 500 nm. Following are characteristic advantages of piezoelectric actuators:

- $<<1$ nm in resolution,
- low inertia,
- fast step possibilities,
- a fast settling time,

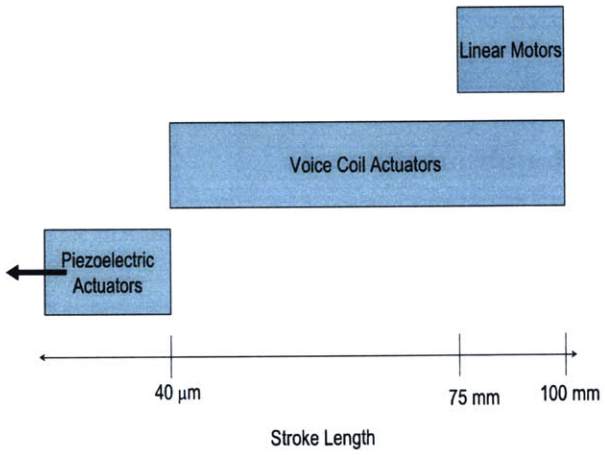

Figure 3-7: Actuator Selection Chart
[7]

- resolution is limited only by noise, and
- no mechanical wear is present

[10]

There are several types of designs from which to choose from: stack design, laminar design, and biomorph type designs (See 3-8). Stack designs consist of a stack of piezoelectric elements separated by metallic electrodes. They expand when a voltage is applied. Laminar design actuators consist of thin ceramic strips. The voltage is applied perpendicular to the the direction of polarization – this means that these actuators contract in response to a voltage. Biomorph designs contain a piezoelectric element attached to a metal substrate. When a voltage is applied, the actuator bends because the metallic strip does not change in length. [10] Selection of which piezo design to use depends on the geometrical and performance criteria of specific designs.

3.3.4 Feedback Requirements

Only two technologies were identified that could meet the Angstrom resolution requirement: laser interferometry and capacitive sensing.

Laser interferometers work by splitting a monochromatic light beam. Part of the beam is transmitted to a fixed mirror; the other part continues to the object being measured. When the beam recombines, a change in intensity can be measured. This difference in intensity is correlated to the displacement. Laser interferometry is desirable because it can allow for direct measurement of the gap displacement. Feedback, however, is only linear to 2-5 nm [41]. Readings are limited by the medium through which the laser travels and any environmental changes that may occur.

Capacitive sensors measure displacement by correlating the potential differences of two surfaces of known dimensions to the gap size. Their ability to sense displacement is limited only by the noise present in the amplifier that they are connected to. Capacitive sensors are also linear to approximately 0.01%. The disadvantage of this method is that indirect measurement of the gap will have to be utilized.

Capacitive sensors are selected for this project because they provide better linearity,

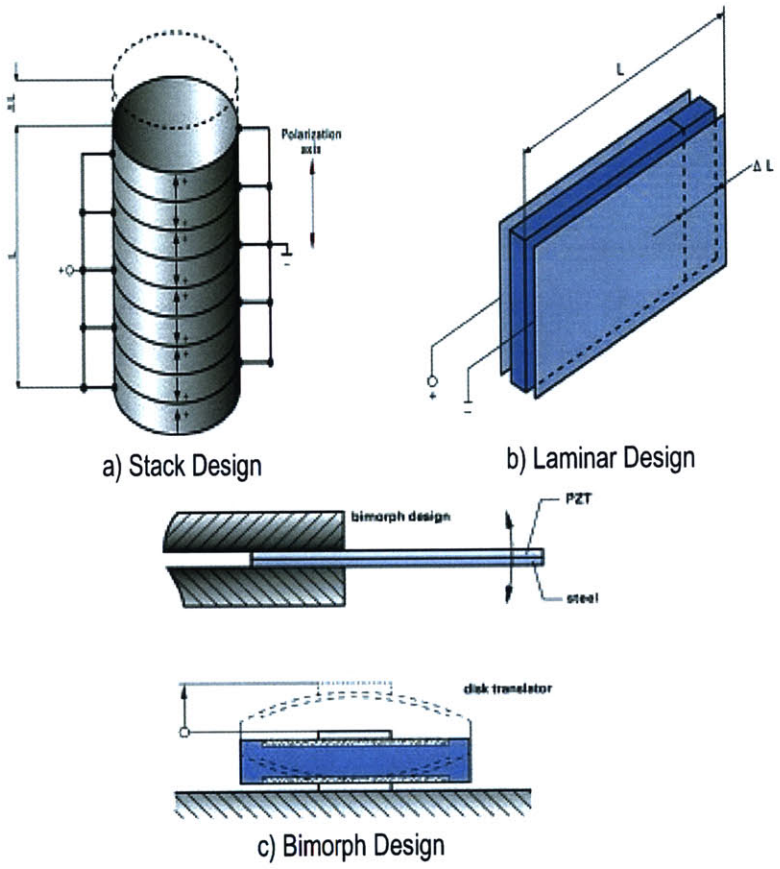

Figure 3-8: Piezoelectric Actuator Design Types
Courtesy of Physik Instrumente (PI) GmbH & Co. KG [10]

and are less sensitive to environmental changes.

3.4 Problem 3 – Fluid Dynamics

The most difficult portion of this project will most likely be obtaining and maintaining an adequate flow rate. Although this will be less of an issue when multiple valves are coupled, the challenge of moving a particle through nanometer sized gaps is still significant. This project is limited in that the flow must be mechanically pumped. This section will describe the fluid-solid interface and fluid movement.

3.4.1 Surface Tension

There are two forces acting when a liquid comes into contact with a solid surface: cohesive forces and adhesive forces. Cohesive forces are the intermolecular forces that keep the liquid molecules together. Adhesive forces are those between the molecules on the outside layer of the liquid and their container. Energetically, the molecules on the surface are in an unfavorable position. The cohesive forces, therefore, pull the surface molecules inward in an attempt to reduce the surface area. This phenomenon is called surface tension. (See Figure 3-9)

A relevant phenomenon occurs when the adhesive and cohesive forces are both strong (in particular for polar molecules such as water) – capillary fluid flow occurs. The most common example of this phenomenon is the rise of water due to capillary action (See Figure 4). The surface tension of water at room temperature is 72 x 10^{-3} N/m at room temperature. This effect may be used to move the fluid through the small gaps.

3.4.2 Fluid Flow

In addition to the surface-liquid interaction, the flow needs to be characterized. The Reynolds number is a ratio of the inertial forces to the viscous forces of the fluid. It is the primary dimensionless parameter that determines the nature of the flow. It is given by:

$$\mathrm{Re} = \frac{\rho_m DU}{\mu_{viscosity}} = \frac{inertia}{viscosity}$$

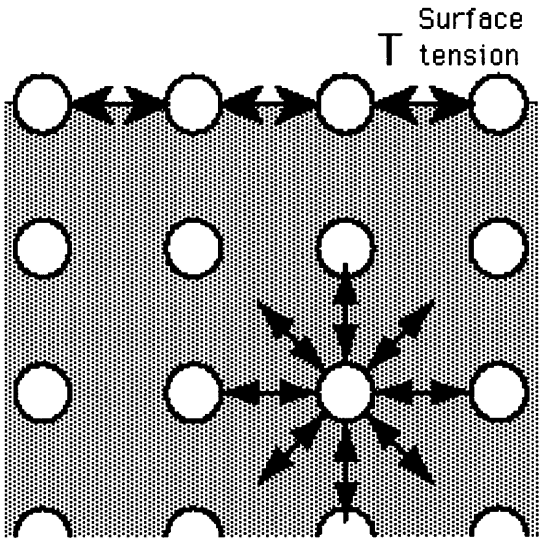

Figure 3-9: Surface Tension
Courtesy Hyperphysics website [25]

Variable Definitions

Re = Reynold's Number

ρ = fluid desity ($\frac{kg}{m^3}$)

D = Characteristic Dimension (m)

U = Velocity($\frac{m}{s^2}$)

μ = viscosity (Pa s)

In general if Re<<1, viscous forces dominate the flow and inertial forces can be ignored. For Re <1000 the flow also tends to be laminar, meaning that it follows smooth streamlines.

Given the desired gap range, the flow will be laminar and viscous forces will dominate. Because viscous forces dominate, the flow will only move when a pressure gradient is present. Once the pressure gradient disappears, the flow will come to a halt almost instantaneously.

There are two ways to model the fluid flow: either by analyzing the fluid as a collection of molecules or as a continuum. To simplify analysis, the continuum model shall be used. This is valid in that a large amount of molecules are present even for small volumes (roughly

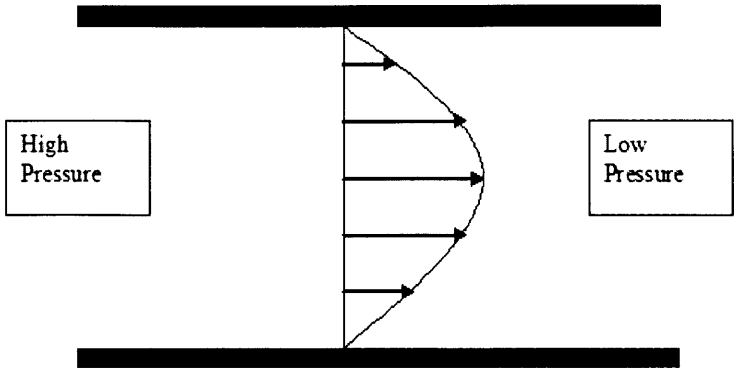

Figure 3-10: Poiseuille Flow

above 20 nm). Although, the fluids to be separated may not be newtonian (a fluid where the strain rate is proportional to the sheer stress), a newtonian fluid will be assumed for simplicity. The flat sections will be fixed. The flow will be assumed to be fully developed with no slip at the boundaries (this may not hold for gaps smaller than 10 nm).

With these assumptions, the flow can be modelled as Poiseuille Flow (See Figure 3-10). The volumetric flow rate can then be found by:

$$Q = \frac{Wh^3}{12\mu_{viscosity}} * \frac{dP}{dx}$$

Variable Definitions

Q = flow rate (m^3/s)

W = Gap width (m)

h = gap height (m)

μ = viscosity (Pa s)

$\frac{dP}{dx}$ = Pressure Gradient $(\frac{Pa}{m})$

Acceptable flow rates for this device is in the range of 10 - 20 μ L/min. One can readily see the difficulty of achieving a good flow rate with one gap. The flow rate is proportional to the gap opening cubed!

Note that it is unclear when the no-slip condition fails. The thin-film properties may be significantly different from bulk properties (most importantly viscosity!!).

3.5 Problem 4 – Biological Compatibility

All materials interfacing with biological samples must be biologically and chemically inert. This means two things: the sample must not extract particles from the interfacing surfaces, and adhesion of the sample to the surfaces must be minimized. Particle extraction from the surfaces would compromise the integrity of the sample. Adhesion or adsorption of the sample by the interfacing surface would result in biofouling(clogging), and possible contamination of future samples. Many coatings are available that prevent extraction of particles by the sample. Adsorption (particularly of proteins), however; is a more difficult problem.

Several factors are believed to be the cause of the protein adsorption. Among them are low surface roughness, surface charge, surface energy, crystallinity, and protein concentration (with surface free energy being the most important) [22]. Interfacial free energy between water and the substrate is used to predict protein adhesion. Hydrophobic materials tend to attract proteins more than hydrophillic surfaces [13]. A possible criteria for an acceptable surface could be that the interfacial free energy between water and the substrate be 1 ~ 3 mJ/m^2 [22]. Coatings of Polyethylene Oxide (PEO) and Polyethylene Glycol (PEG) have been found to reduce protein adhesion and are the best available coatings at this time [22] [50] [35] [5] [29]. Application of PEG is not the final solution because it will only reduce the amount of non-specific adsorption – not completely eliminate it. As a result, the surface will not be biocompatible for an extended period of time. The exact life span of the coating has will need to be experimentally determined.

3.6 Problem 5 – A Cost Effective Design

Because biological compatibility is expected to deteriorate over time, to fully comply with the requirement of a compatible surface the interfacing surfaces must cleaned or replaced. Replacement is a more desirable solution at this time.

Cleaning the interfacing surfaces of an assembled product is not a realistic solution

at this time. Sending a cleaning agent through the gap may not sufficiently remove the adhered molecules. A heat clean will most likely distort the surface flatness and roughness. Electrical cleaning may polarize the interfacing surfaces and attract more adhesion. Direct access to the surfaces may allow sufficient cleaning by mechanical removal of compromised surfaces.

Disposability solves the biological compatibility deterioration issue but creates the problem of needing a cost effective design. The costs can be broken down into manufacturing and equipment costs. Manufacturing costs can be reduced by minimizing the production steps of the machine. Equipment costs can be kept low by modularizing the design. This keeps reusable equipment separate from necessarily disposable parts. Reusable equipment include pumps, actuators, and sensors.

3.7 Comparison of Valve Designs

The valve designs presented at the end of Chapter 2 do not fully meet the requirements of this project. All designs minimize an initial gap size, use a piezoelectric actuator, and provide an isolated environment for fluid flow. The reasons that the unmodified designs do not meet the requirements of this project are presented below.

3.7.1 The Nanogate Design

An unmodified adoption Nanogate is not acceptable because it lacks:

- An acceptable sensing mechanism,
- A guarantee that the two surfaces to create the gap remain parallel as the gap size is increased, and
- Biological compatibility

3.7.2 The JPL Design

An unmodified JPL microvalve design is not acceptable because it lacks:

- A guarantee that the two surfaces that create the gap remain parallel as the gap size is increased,
- A non-integrated actuation and sensing system,
- Biological compatibility,

3.7.3 The Tubular Valve Design

An unmodified adoption of the Tubular Filter is unacceptable because it lacks:

- A guarantee that the two surfaces to create the gap remain parallel as the gap size is increased,
- Materials that satisfy thermal requirements for stable control of the gap size, and
- Biological compatibility

3.8 Chapter Summary

This chapter refined the user requirements for a technology. It specifically described challenges towards creating a gap 0.5 nm in height, controlling the gap, adequate fluid flow, biological compatibility, and modularization of the design. Three valve designs for consideration were shown to need modification to meet the design requirements.

Chapter 4

Proposed Design Solution

4.1 Introduction

Chapter 2 described technologies and methods used for separating biologically active molecules. The case was made for pursuing a size based approach using valve technology. Chapter 3 detailed the technical criteria for any design and established reasons for not adopting the presented valves.. This chapter presents a design for addressing the challenges presented in the previous chapters.

4.2 Design Overview

A cross-sectional view of the proposed concept is shown in Figure 4-1. It is a design based on the JPL valve. The base is essentially the same. It contains the inlet and outlet. Rings and valleys have been removed to provide a flat surface. The diaphragm, on the other hand, was modified by adding a pivot at the center. The pivot was added to compensate for any tilt between the two flat surfaces prior to initial mating (See Figure 3-6). Epoxy is inserted at the pivot when the two flat surfaces initially meet. This ensures that the plates stay parallel as the force on the diaphragm is reduced to create the desired gap size. The midsection and base are joined together to maintain a well defined environment for fluid flow. The top portion of the design now holds a ring stack actuator instead of a solid stack. A capacitive sensor is held at the center of the ring. The top mates with the base

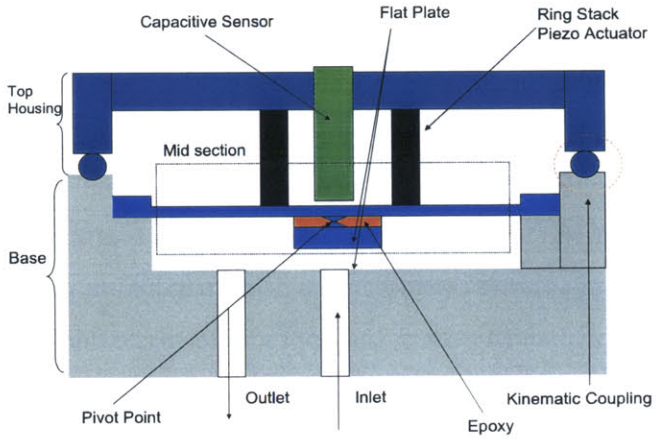

Figure 4-1: Modified JPL Valve

by means of a kinematic coupling to provide modularity between the flow environment and the actuation/sensing system.

4.3 Prototype Material Selection

4.3.1 Structural Materials

The materials for the prototype must be able to produce a well designed diaphragm, pivoting flexure, as well as a stable structure. The following properties are relevant to selection:

- Yield Strength,
- Modulus of Elasticity,
- Hardness,
- Ductile materials preferred over Brittle Materials,
- Coefficient of Thermal Expansion, and
- Workability (easy to machine or manufacture)

Chart 4.1 presents several materials for consideration. From a final product standpoint, silicon is the more desirable material. From a prototype standpoint, Aluminum is the material of choice.

Silicon is well known for nearly negligible hysteresis and there is much ongoing research concerning biocompatibility. It is brittle and stiff. A working prototype made out of silicon would best be manufactured by microfabrication methods which places the size scale of the machine in the micron to millimeter range. This is more costly and difficult than conventional manufacturing because of the detail required in planning the fabrication process and the cost of manufacturing the appropriate masks for this design. Without experimental validation that the concept will work, it is best to seek a material that is easier and less costly to machine. A micromachined silicon valve is the next step in this research pending experimental characterization of a prototype.

Aluminum 7075-T6 was chosen for building the prototype because it is easy to machine, meets the rigidity requirements of the base and top housing, while maintaining the flexibility for the diaphragm. Its properties sufficiently allow for valuable insight to the pros and cons of the design. Scale of an apparatus built out of aluminum forces features of the machine to a millimeter to centimeter size scale.

The disadvantage of using Aluminum is that the material itself can not be used to achieve a surface flat enough to the necessary specifications of this project. The only clear advantage of the design at this scale over a MEMS scale design is coating for biological compatibility. The reason for this is that this particular prototype design does not require any heat in its fabrication, assembly can be done through bolts, screws, and/or adhesives. Heat could degrade and release the PEG coated on a surface. Much research is underway, however, that seeks to address this issue.

Two Aluminum 7975-T6 4" diameter and 1" thick stock disks were purchased from McMaster Carr for the base and top portion. A 3" diameter and 0.75" thick stock plate was purchased for manufacturing the diaphragm.

Material	Yield Strength	Modulus of Elasticity	Compressive Yield Strength	Poisson's Ratio	Ductile /Brittle	Hardness	Coefficient of Thermal Expansion	Manufacturing Methods
Aluminum 7075	505 MPa	72 GPa	---	0.33	Ductile	191 kg/mm^2 (Knoop)	23.6 $\mu m/m^oC$	Conventional
Fused Silica	55 MPa (Apparent)	73 GPa	1108 MPa	0.17	Brittle	500 kg/mm^2 (Knoop)	0.54 $\mu m/m^oC$	Microfabrication
Silicon (Single Crystal)	21 GPa	130 GPa	500 MPa	0.18	Brittle	2480 kg/mm^2 (Knoop)	2.30 $\mu m/m^o C$	Microfabrication

Table 4.1: Selected Material Properties

4.3.2 Flat Plates

Because the suitable flatness for testing can not be achieved with Aluminum, a separate surface is needed to create the gap. Slots shall be cut in the base and rigid center of the diaphragm for attaching flat surfaces. Six Fused Silica plates with 1/10 wave flatness were purchased from Cymas Optical in Massachusetts. The flatness corresponds to a peak to valley height of no more than 60 nm on each plate. Dimensions of the plates are 10 mm x 10 mm x 3 mm. Three of the flat plates contain a 0.25 inch center hole (to be used in the slot in the base). No dimensional analysis will need to be performed on the flow because these plates create a gap on the order of the desired final product.

4.3.3 Coating

Initial testing will not be done on biological samples. Polystyrene latex spheres were purchased for filtration tests. As a result, a water resistant coating is the only thing needed. PDMS was chosen as the coating to be placed on the aluminum. The fused silica need not be coated. The spheres may stick to the Fused Silica, but can be removed by washing in distilled water.

4.4 Base Design

The base contains two 0.25 inch holes for attaching tubes that serve as the inlet and outlet of the flow. At the center of the base is a slot for inserting a flat plate. Sealant is to be placed around the Silica plate to ensure that the only pathway for a fluid to flow is through the gap created when the base and midsection are joined. Figure 4-2 shows the base assembled with the flat plate in the center.

4.5 Midsection Design

The midsection is perhaps the most critical part of the design. It holds a flat plate at the center. This flat plate is the top boundary of the desired gap. All motion for controlling gap size and tilt compensation happens here.

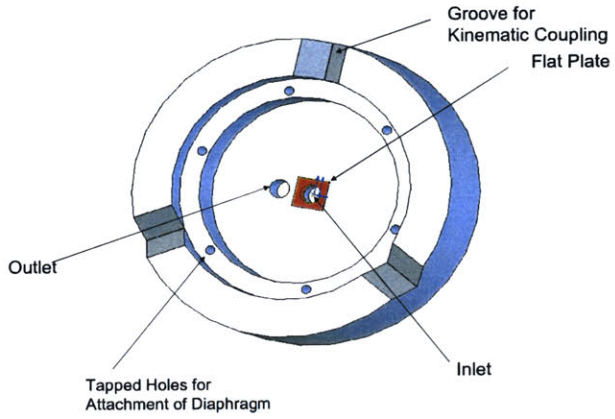

Figure 4-2: Base – Prototype

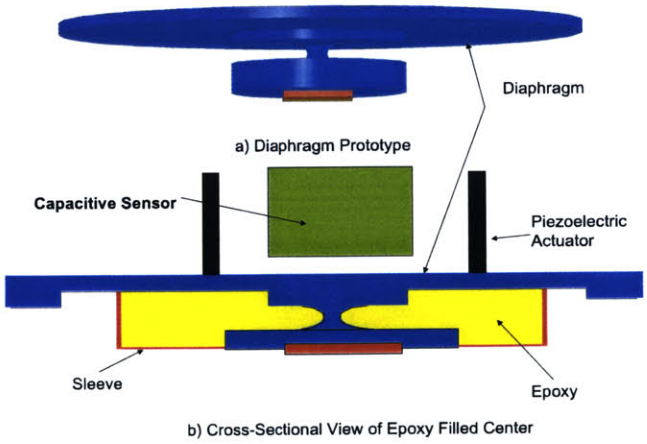

Figure 4-3: Midsection – Prototype

This portion of the design can be thought of as a diaphragm with a rigid center. In the worst case scenario, the diaphragm should vertically deflect at least 10 μm for 800 N (the sensing limitation of the capacitive sensor and the maximum load the piezoelectric actuator can apply). Plastic deformation must not occur and hysteresis must be minimal.

Design of the midsection does not end with the diaphragm. Tilt compensation is also required. This problem is addressed by placing a pivot at the center of the diaphragm. The pivot is to deflect upon the mating of the two flat surfaces so that the two surfaces become parallel. A human hand should be able to move it rotationally but not longitudinally. This requirement is set so that the flat plates not be stressed. To ensure that the plates remain parallel, an epoxy will be inserted through holes in the diaphragm after it has tilted. The epoxy will be contained within a sleeve made out of PDMS (polydimethyl siloxane) that surrounds the pivot. The epoxy chosen for this must be of low viscosity prior to insertion and stiff upon completion of cross-linking. Figure 4-3 shows the mid-section with a flat plate attached at the bottom and a cross-sectional view of the part with the sleeve and epoxy included.

4.5.1 Physics of a Diaphragm

A diaphragm can be thought of as a flat circular plate (the thickness is no larger than $\frac{1}{10}$ of the length of the smallest lateral dimension [33]). The equations for a concentrically loaded and fixed at the ends plate follow [33]:

Please Refer to Figure 4-4)

Given:

$$W = \frac{Load}{2a_1\pi}$$

$$\beta = \frac{a_1}{a_L}$$

$$\alpha = \frac{r}{a_L}$$

$$D = \frac{Eh^3}{12(1-\nu^2)}$$

$$C_1 = (1-\beta^2) + 2\beta^2 ln\beta$$

$$C_2 = (\beta^2 - 1) - 2\ln\beta)$$

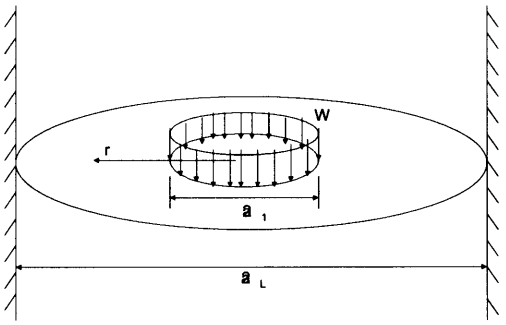

Figure 4-4: Diaphragm Model

If $\alpha \leq \beta$:

$$w = \frac{Wa_L^2 a_1}{8D}(C_1 - C_2\alpha^2)$$

If $\alpha \geq \beta$:

$$w = \frac{Wa_L^2 a_1}{8D}[(1+\beta^2)(1-\alpha^2) + 2\beta ln\alpha + 2\beta^2 ln\alpha + 2\alpha^2 ln\alpha]$$

Variable Definitions

W = Load per circumference (N/m)

β = ratio of load radius to diaphragm radius

α = ratio of radial position from center of diaphragm to diaphragm radius

D: Fexural Rigidity

E: Young's Modulus (N/m^2)

ν = Poisson's Ratio

A look at the constant $\frac{wa_L^2 a_1}{8D}$ reveals that deflection is greater for higher load, low flexural rigidity, and large diameters. Adding a mass (pivot diameter) to the center should have the effect of stiffening the diaphragm, thus decreasing the range of motion.

4.5.2 Physics of the Pivot

The design of the midsection does not end with an analysis of the diaphragm. A compliant mechanism is also required for tilt compensation. The pivot is required to be rigid along the longitudinal axis while the remaining two axes are to be compliant. Two options exist to accomplish this (See Figure 4-5):

1. two single axis flexures at right angles to each other, or
2. a circular flexure

The circular flexure was chosen because of manufacturing ease. In order to ensure that the concept is valid, an examination of the solid mechanics of the pivot is examined. The exact equation for angular compliance of a solid revolute pivot is given as follows [30]:

Variable Definitions

Please refer to Figure 4-6 to get a better picture of these variables

α: deflection about z axis

t:thickness (m)

h: largest diameter of pivot (m)

F: applied force (N)

R: Radius of Curvature of Pivot

E: Young's Modulus

$\beta = \frac{t}{2R}$

$\gamma = \frac{h}{2R}$

Δx = change in longitudinal dimension

$$(\frac{\alpha_y}{M_y})_{ta} = (\frac{\alpha_z}{M_z})_{ta} = \frac{\alpha_z}{F_y R sin\theta_m} = \frac{\alpha_y}{F_z R sin\theta_m}$$

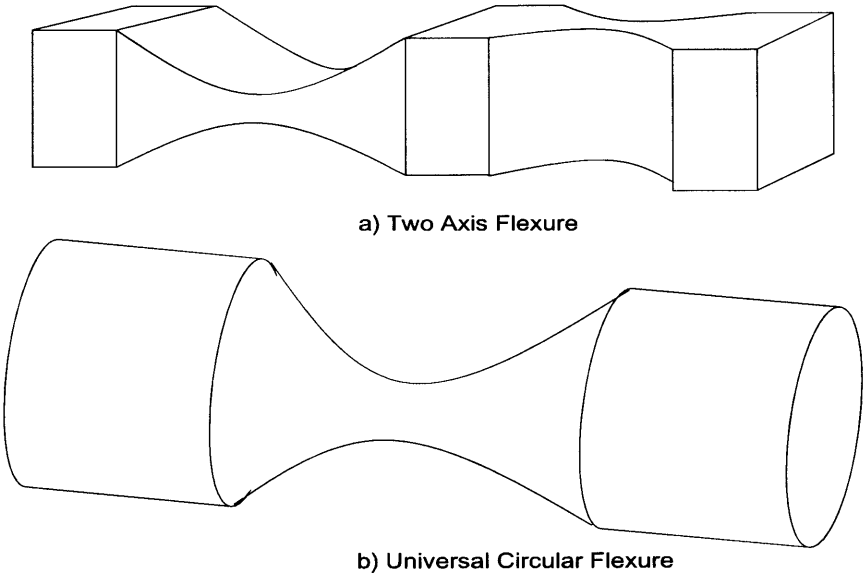

Figure 4-5: Flexure Options

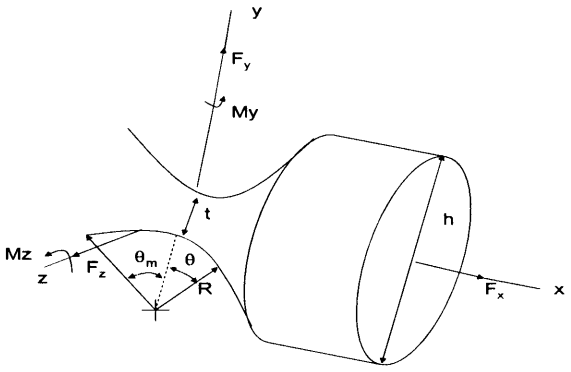

Figure 4-6: Hinge Dimensions and Forces

$$= \frac{8}{3\pi ER^3(2\beta+\beta^2)} \times \{[\frac{1+\beta}{\gamma^3} + \frac{2(1+\beta)^2+3}{2\gamma^2(2\beta+\beta^2)} + \frac{2(1+\beta)^3+13(1+\beta)}{2(2\beta+\beta^2)^2\gamma}] \times \sqrt{1-(1+\beta-\gamma)^2} + \frac{12(1+\beta)^2+3}{(2\beta+\beta^2)^{\frac{5}{2}}} \times [tan^{-1}\sqrt{\frac{2+\beta}{\beta}} \frac{\gamma-\beta}{\sqrt{1-(1+\beta-\gamma)^2}}]\}$$

Simplified, the equation approximates:

$$(\frac{\alpha_y}{M_y})_{ta} = (\frac{\alpha_z}{M_z})_{ta} \approx \frac{20}{ER^3(2\beta)^{\frac{7}{2}}} = \frac{20R^{\frac{1}{2}}}{Et^{\frac{7}{2}}}$$

Longitudinal compliance is given by:

$$\frac{\delta x}{F_x}_{ta} = \frac{2}{\pi ER}\{[\frac{2}{(2\beta+\beta^2)^{\frac{3}{2}}} \times tan^{-1}\sqrt{\frac{2+\beta}{\beta}} \frac{\gamma}{\sqrt{1-(1+\beta-\gamma)^2}}] + [\frac{(1+\beta)}{(2\beta+\beta^2)\gamma}\sqrt{1-(1+\beta-\gamma)^2}]\}$$

which approximates to:

$$\frac{\Delta x}{F_x}_{ta} \approx \frac{2}{ER(2\beta)^{\frac{3}{2}}} \approx \frac{2R^{\frac{1}{2}}}{Et^{\frac{3}{2}}}$$

From the simplified equations, one can determine that both angular and longitudinal compliance can be lowered by reducing the modulus of elasticity or the thickness where bending is to occur.

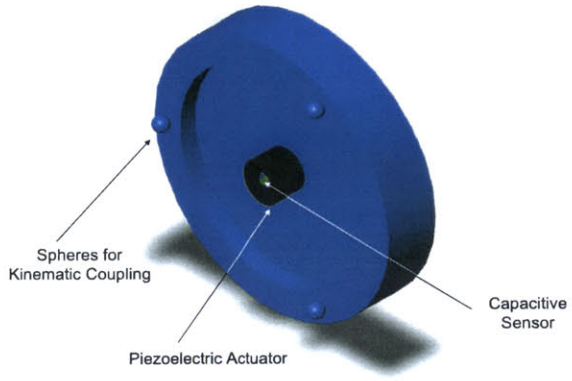

Figure 4-7: Top Housing – Prototype

4.5.3 Machining Considerations

Diaphragm diameter shall be the smaller stock diameter of the purchased aluminum (3mm). In terms of the lowest machinable thickness, the limit is 1 mm using a lathe. Machining below a 1 mm thickness is difficult because the piece is not easy to secure and vibrations affect the quality of the part. An FEA study was performed to consider fabrication of a diaphragm with a non-constant thickness. The studies showed that the 1 mm thickness was still required but did not have to span the entire cross-section.

4.6 Top Housing

The purpose for the top housing is to hold both the piezoelectric actuator and capacitive sensor. The actuator will be attached by means of an epoxy. The capacitive sensor will be placed and held inside the actuator with a split ring (See Figure 4-7).

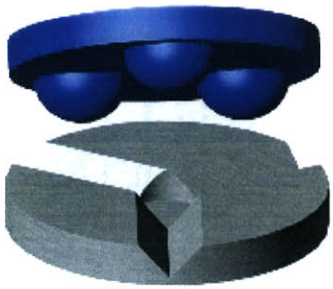

Figure 4-8: Kelvin Clamp Kinematic Coupling
Courtesy of Alex Slocum [36]

4.7 Assembly of Base and Top Housing

Because the base and top housing need to join in order valve to function, a reliable method of joining the two parts must be in place. Errors due to disassembly and reassembly must be minimized.

Kinematic couplings are one way of approaching this problem. The idea of a kinematic coupling is to rigidly fix the bodies of the system in relation to each other without any over constraint. The Kelvin clamp (see Figure 4-8) will be the kinematic coupling used for this project: an equilateral triangular arrangement of spheres on one component and v-grooves on the other component. This coupling provides six contact points which result in the constraint of all six degrees of freedom (3 translational and 3 rotational). Stability is ensured by making the normals to the plane of the contact forces bisect the angles of the spheres sitting in the grooves (for more information on Kinematic Couplings and their design please see reference [36]).

4.8 Actuation and Sensing

On initial assembly of the valve, the two flat plates are a distance apart and not parallel. When the piezoelectric actuator expands it will deform the diaphragm and bring the flat plates closer. The sensing system must be able to detect when the flat plates meet and are

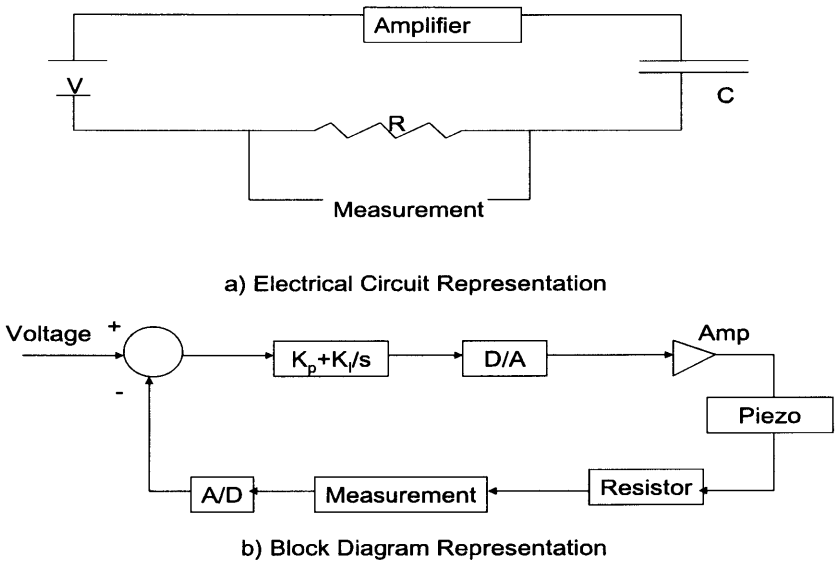

Figure 4-9: Graphical Representations For Sensing Closure of the Gap

parallel and it must be able to determine the amount of deflection the diaphragm has been subjected to. This data will allow for a size selectable gap.

4.8.1 Initial Sensing System

Piezoelectric actuators store energy in the coupled form of an electrical charge (Voltage) and a mechanical strain. The opposite also holds true, when a force or pressure is applied to a piezo, it stores energy in the form of strain and charge. It happens that that the voltage applied is proportional to the expansion of the actuator.

Because the load changes when the plates fully mate, is anticipated that a current change shall occur. By monitoring the system for this current change through a resistor attached to the actuator, one can know when the plates have become parallel (See Figure 4-9).

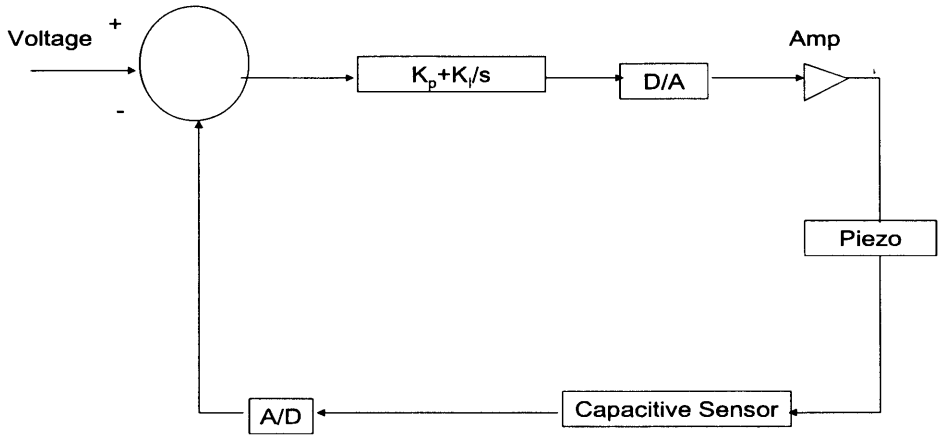

Figure 4-10: Block Diagram of Sensing with Capacitive Sensor

4.8.2 Gap Height Sensing

Once it has been determined that the system has closed the gap, all sensing is then performed by the capacitive sensor (see Figure 4-10). Instead of measuring a current change, feedback in this system is provided through a voltage signal.

4.8.3 Piezoelectric Actuator Technical Specifications

The actuator was purchased from Polytec PI (model number P-306.10). It has a 8 mm inner diameter, 16 mm outer diameter, its length is 12 mm. The stroke is 10 microns with a maximum push force application of 800 N. In addition to the piezo, an amplifier was also purchased for its operation (model number E-461.00).

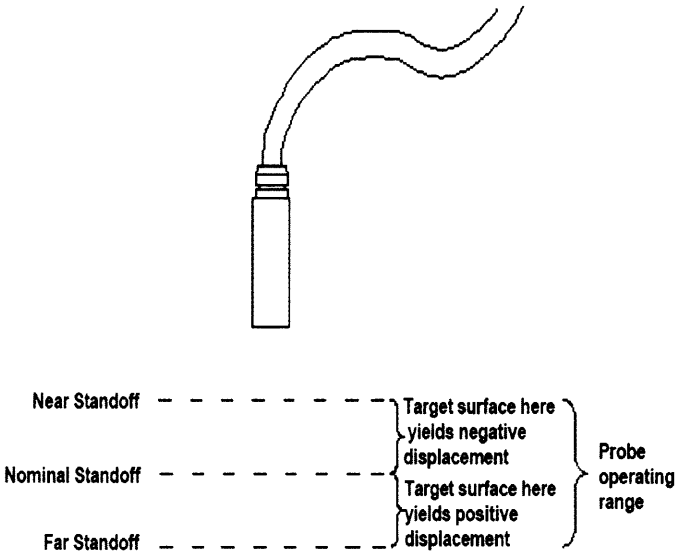

Figure 4-11: How the Probe Measures Displacement
Picture Courtesy of ADE Technologies

4.8.4 Capacitive Sensor Technical Specifications

A capacitive sensor (2.64 mm diameter, 13.2 mm length) was purchased from ADE Technologies. The probes measure variations of the distance from a nominal position (See Figure 4-11. Output is provided for a displacement range of +/- 10 μm. Resolution is 0.10 nm. The output voltage is given for a range of +/- 10 V.

4.9 Fluid Control

It is important that the system that moves the fluid not contaminate the fluid. For this reason, peristaltic pumps were determined as the method of moving the fluid along with silicone tubing. The specification for the purchases are presented below.

4.9.1 Pumps

Two peristaltic pumps were purchased to move the water and latex spheres. One pump was purchased from VWR. It is a bidirectional pump with a flow rate ranging from 4 to 85 $\frac{ml}{min}$. A suction only Barnant E-Series pump was also purchased with a flow rate of 375 $\frac{ml}{min}$.

4.9.2 Tubing

Silicone tubing was selected because it best meets the requirements for peristaltic pump use, biocompatibility, and the range of temperatures in which it can be used [18]. The tubing was purchased from VWR.

4.10 Chapter Summary

This chapter presented a diaphragm valve design concept for the separation of biologically active molecules. It presented a discussion of the specifications for each component of the design along with any relevant physical explanation.

Chapter 5

Simulations, Experiments and Results

5.1 Introduction

This chapter seeks to demonstrate that the concept presented in Chapter 4 will work. Experiments were performed to characterize the design according to controllability, ability to compensate for tilt, and overall adherence to designed parameters(stiffness,deflection, etc.).

5.2 Diaphragm Design Simulations and Experiments

5.2.1 Diaphragm Finite Element Analysis – Deflections and Stresses

Finite element analysis was used to model the vertical deflection of the diaphragm (see Figure 5-1). A concentric force load of 30 N was applied. The underside edge of the model was fixed. A vertical displacement of 20 microns was predicted to occur at the center of the diaphragm. This is twice the required displacement. Von Mises stress analysis showed that the maximum stress approximates 18.06 MPa for the 20 micron deflection (see Figure 5-2). Roughly an order of magnitude less than the 505 MPa yield stress limit of the material.

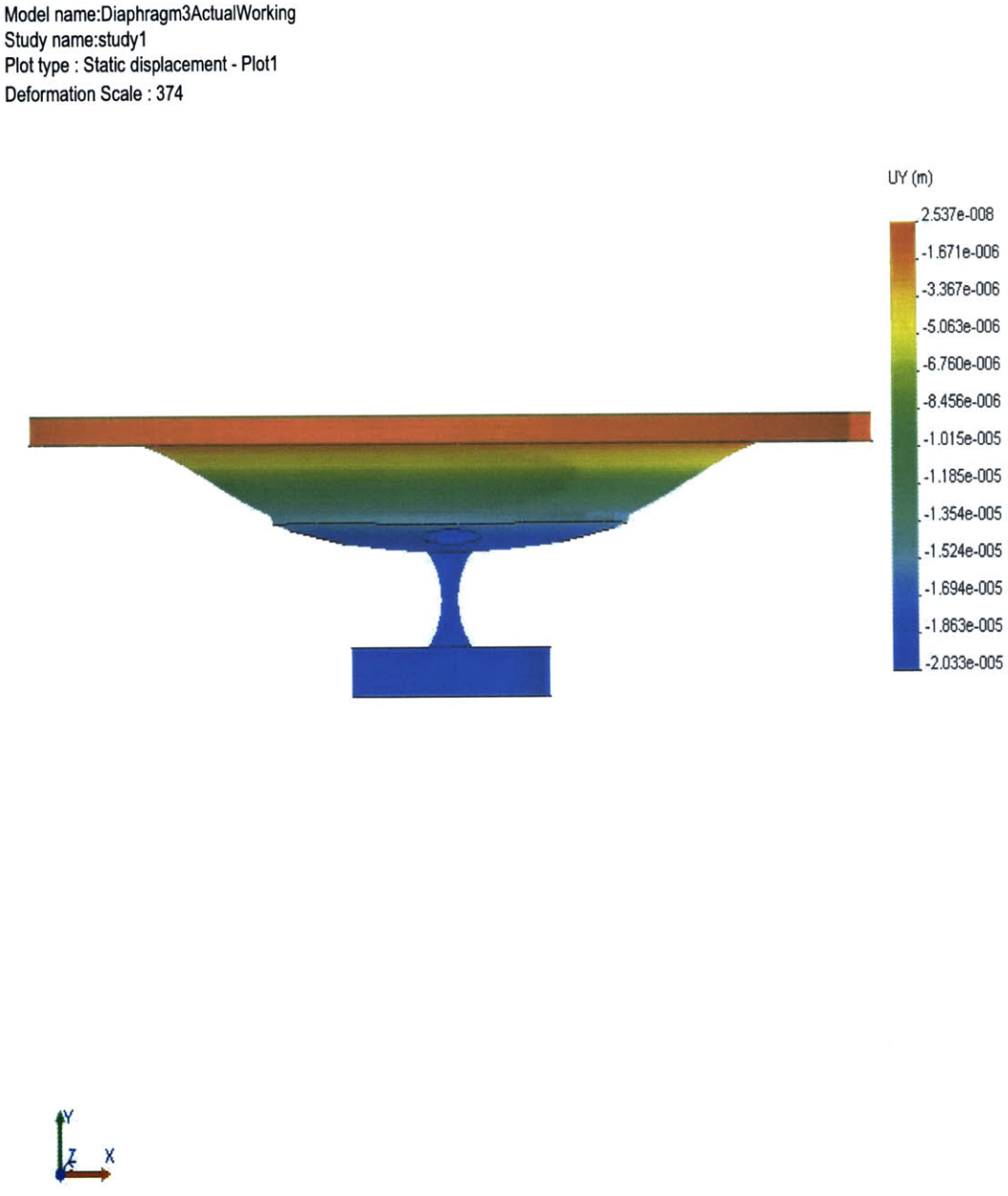

Figure 5-1: Diaphragm (Aluminum 7075) Displacement Study
This diagram is the result of a 30 N concentric load (See 4-4applied at the center of the diaphragm.

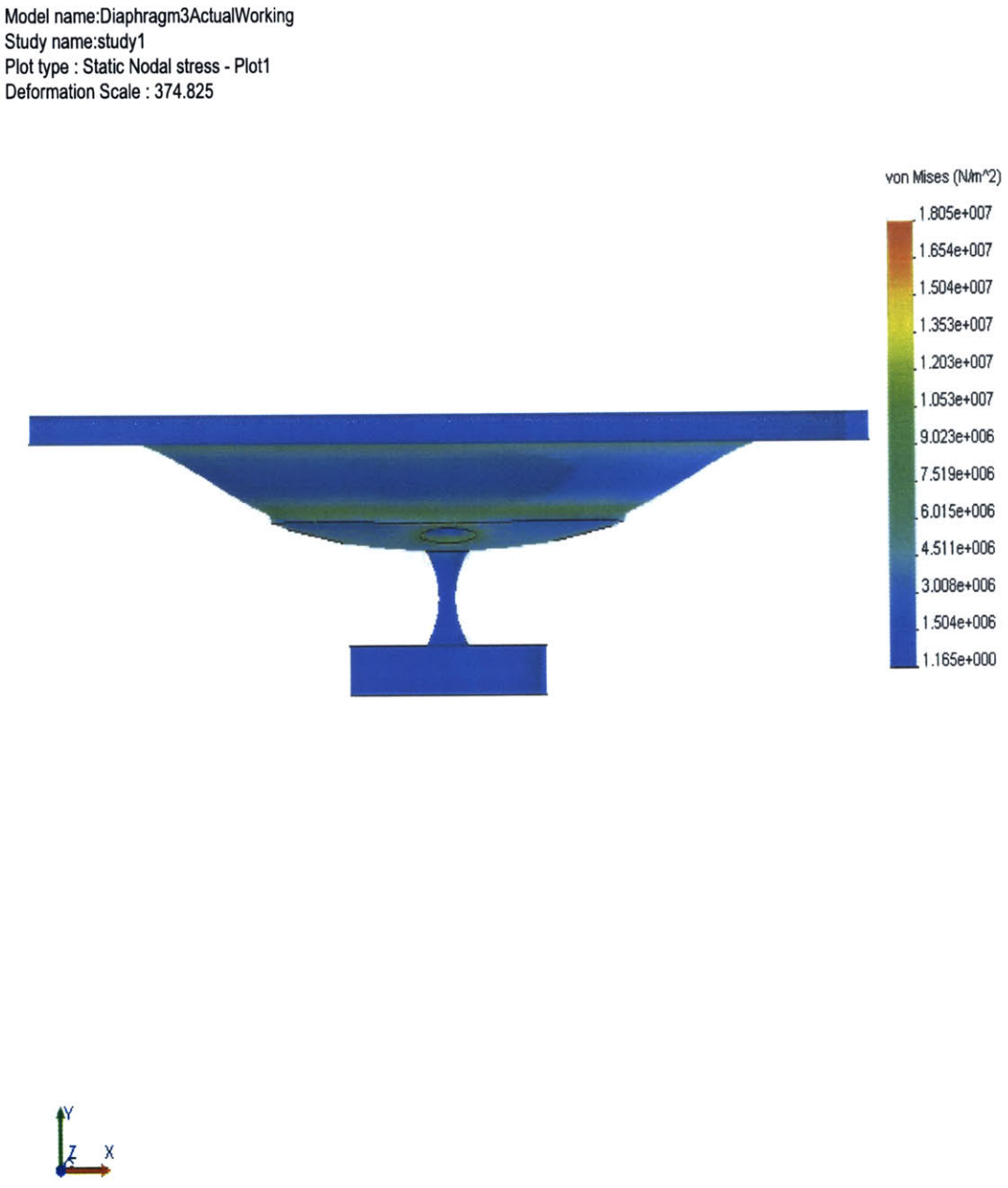

Figure 5-2: Diaphragm (Aluminum 7075) Stress Study
This diagram is the result of a 30 N concentric load (See 4-4applied at the center of the diaphragm.

5.2.2 Diaphragm Stiffness Verification–Experiment Number 1

The simulations were used to design the diaphragm such that it would deflect 20 microns for 30 N (a stiffness of 1.5 $\frac{N}{\mu m}$)of concentrically applied force. A set of weights ranging from 1 g to 50 g (0.001N to 0.5N) were placed at the center of the diaphragm. Deflection was measured by a capacitive sensor placed below the diaphragm. A linear fit approximation of the data(See Figure 5-3) showed that the experimental value of the stiffness was approximately 1.49 $\frac{N}{\mu m}$. This is a difference of of 0.67%.

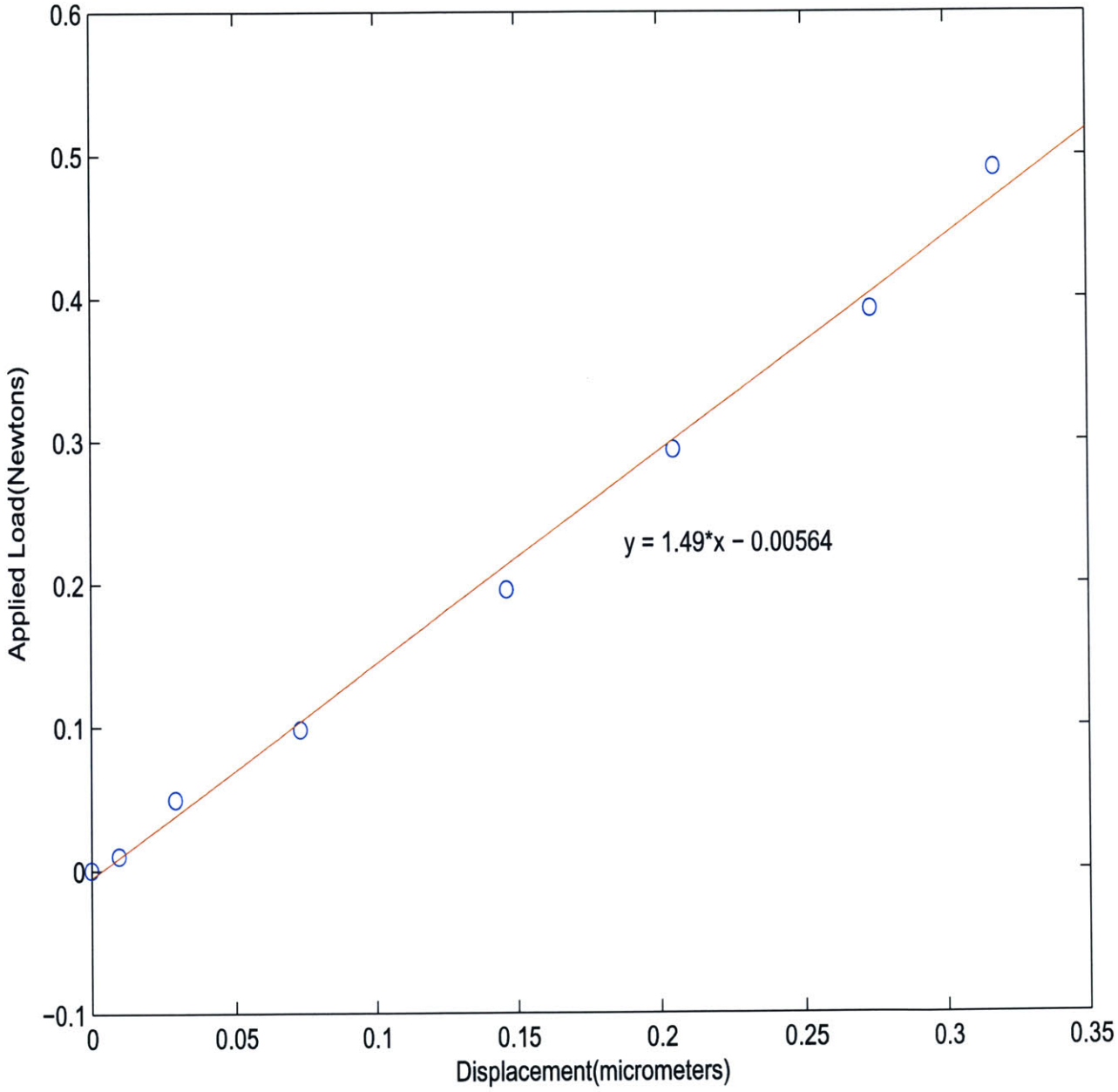

Figure 5-3: Linear Fit of Diaphragm Applied Force vs. Deflection Experiment
For this experiment, weights were placed on top of the diaphragm and deflection was measured via a capacitive sensor.

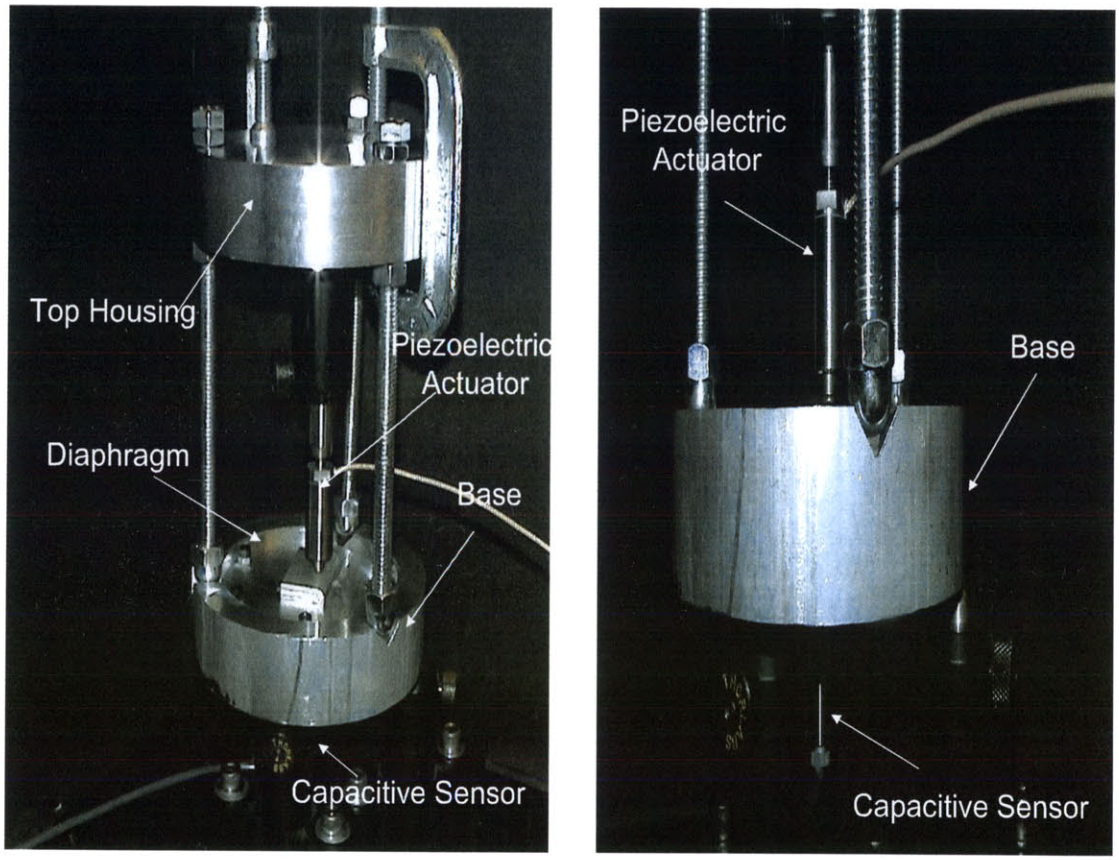

Figure 5-4: Picture of Diaphragm Motion Control Test

5.3 Diaphragm Experiments - Open Loop and Closed Loop Characterization

5.3.1 Open Loop Motion – Experiment Number 2

This test was intended to verify that hysteresis is measurable when the motion of the piezoelectric actuator and diaphragm is in open loop control. Having a means to capture this data can later be used to build a non-linear controller for the valve.

In this experiment, the entire valve is assembled as shown in Figure 5-4. Note that the capacitive sensor is located below the diaphragm and that the piezoelectric actuator used is not annular. Neither the capacitive sensor nor the piezoelectric actuator used for this experiment are specified for the design in Chapter 4. This spare actuator and sensor were used as a precaution. Piezoelectric actuators fracture easily when bending moment or torsion are present. The actuator used is manufactured by Piezomechanik (model number 150/7/20 VS12). The capacitive sensor is probe number 2805 from ADE Technologies.

Using a function generator, a 1 Hz. sine pulse was applied to the piezo. The amplitude of the pulse was 122.6mVPP with a 100 mVDC offset. The amplifier used for the peizoelectric actuator had a gain of 30. Data was captured from an oscilloscope for 5 sine pulses. For the applied voltage, a freely expanding piezo(meaning secured on one end and free at the other) would expand by 0.5 microns (500 nanometers). From this experiment, it was determined that the piezo deflects the diaphragm 0.26 microns. This is total travel loss of 0.24 microns. In addition, there is as much as 1.5% voltage increase through this 0.26 micron travel. The data for one pulse was plotted in Figure 5-5.

5.3.2 Closed Loop Characterization of the Diaphragm – Experiment Number 3

The system was placed in PID closed loop operation for the purpose of determining the smallest recordable change when a step input is applied. A 2mV staircase pulse was applied in increments of 0.5mV (See 5-6). The output was sent through a low pass filter and recorded. Figure 5-7 presents the lowest step output observable – 1.8 nanometers. Too much noise was present at lower step sizes for a reliable measurement. The plot shown

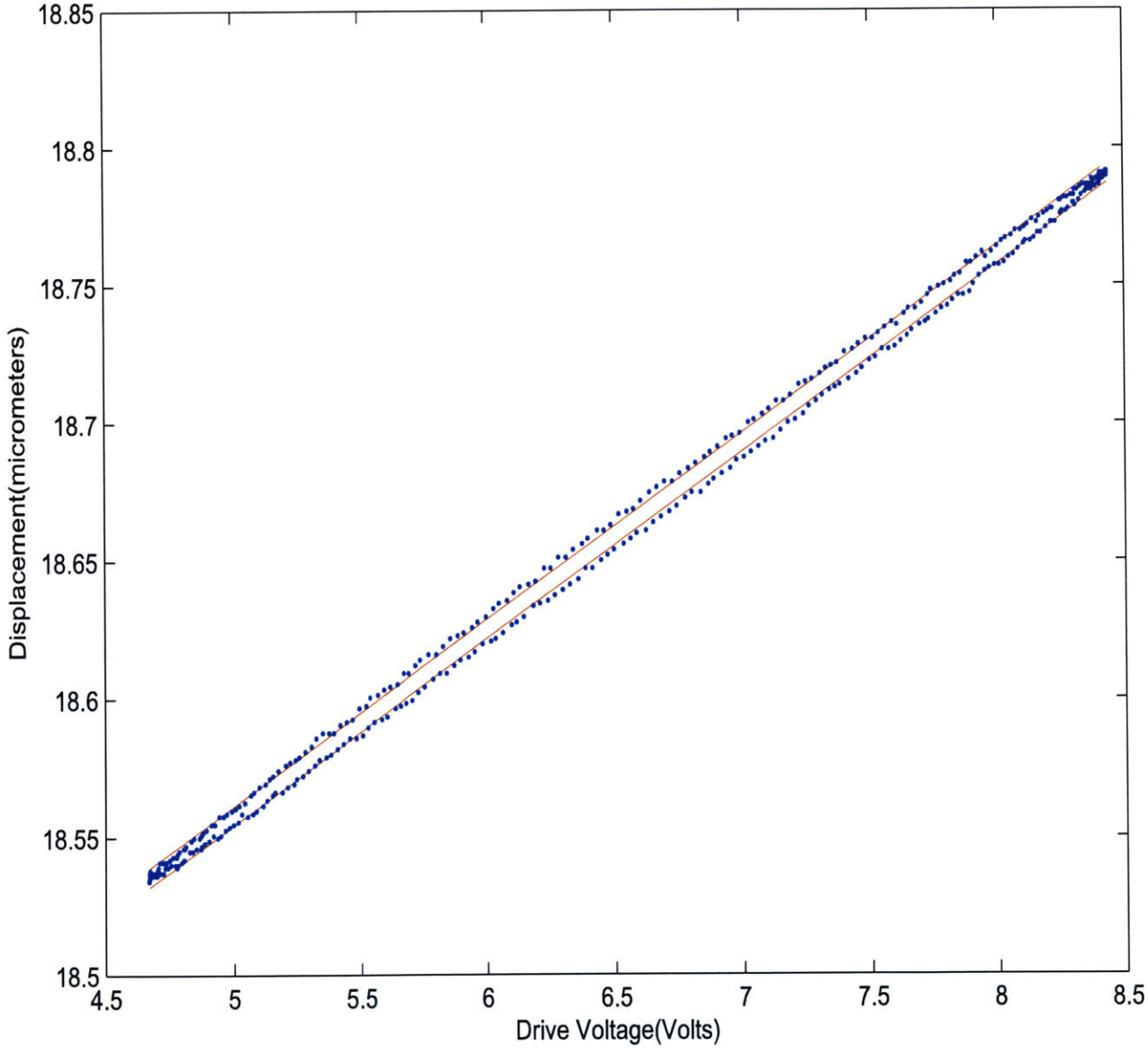

Figure 5-5: Hysteresis Plot of an Open Loop Controlled Design

shows negative displacements because of an offset in the capacitive sensor reading.

5.4 The Tilting Mechanism

5.4.1 Flexure Finite Element Analysis – Deflections and Stresses

Finite element analysis was performed on the pivot for numerical prediction of the compliance. The pivot should be compliant such that it will tilt without damaging the Fused Silica flat plates. A load of 30 N was applied on an edge of the slot created for holding the plates. The resultant displacement is approximately 18 microns at the edge of load placement(see Figure 5-8). Stress is approximately 456 MPa for this applied load, this is close to the 505 MPa yield stress. Plastic deformation of the pivot when the two plates mate and become parallel is not of concern because recovery of initial shape is not desirable.

5.4.2 Visual Verification of Tilting Concept – Experiment Number 4

The universal flexure (See Figure 4-5b) joint was machined out of an Aluminum rod and epoxied to an Aluminum beam. The assembly was secured to one side of a vise. A tilted surface was fixed on the opposing surface of the vise. This set-up simulated the displacement control provided by the piezoelectric actuator. Initial contact occurred at one of edge of the mating area. Once contact was initiated between the mating surfaces, the flexure began to tilt thus making sure that the two surfaces became parallel. Once tilt compensation was completed the vise was moved back and it was observed that the two pieces remained parallel relative to each other. The visual experiment showed that the contact method does force the two surfaces to become parallel (See Figure 5-10). Some spring back was observed and can be seen in the video taken of the experiment. Filling the area with epoxy should eliminate most of the springback.

5.5 Chapter Summary

This chapter presented simulations and experiments relevant to the characterization of the concept presented in Chapter 4. It was shown that manufactured components adhered to

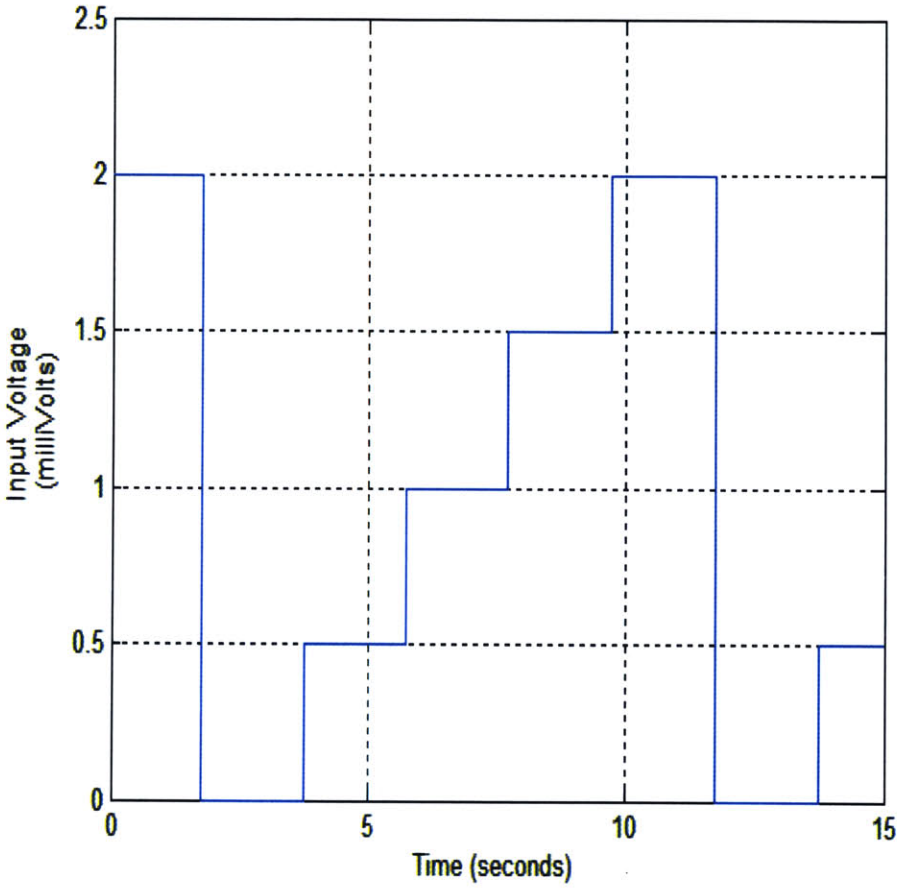

Figure 5-6: Closed Loop Input Actuation Pulse

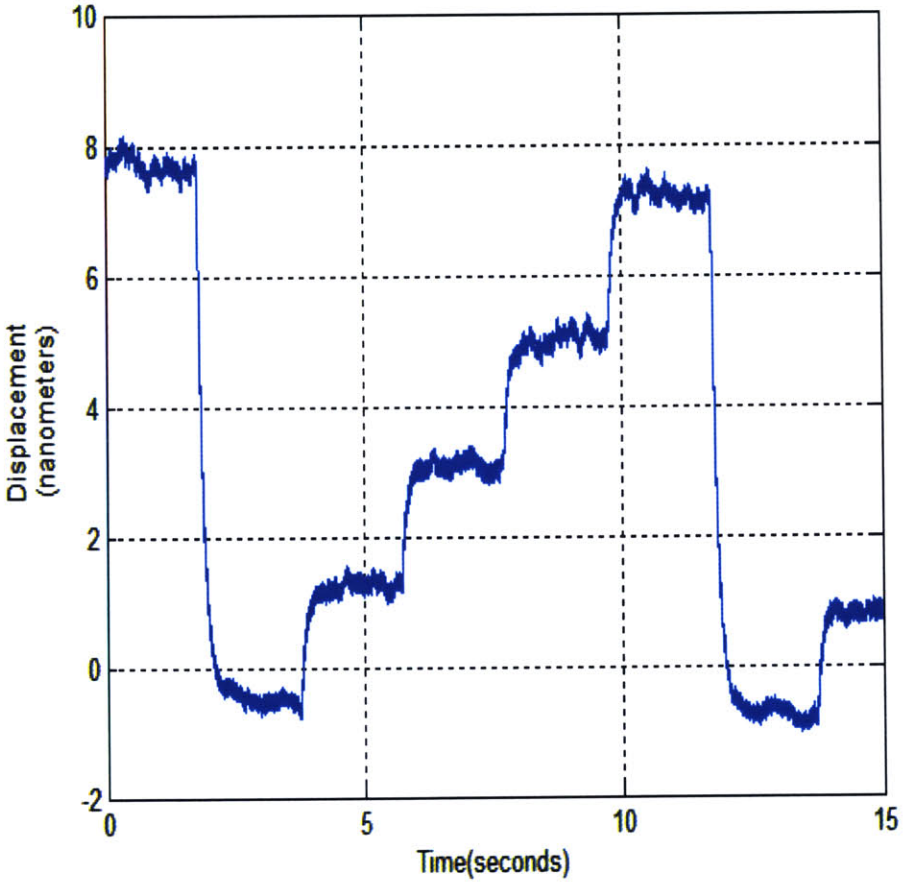

Figure 5-7: Closed Loop Output Actuation Pulse

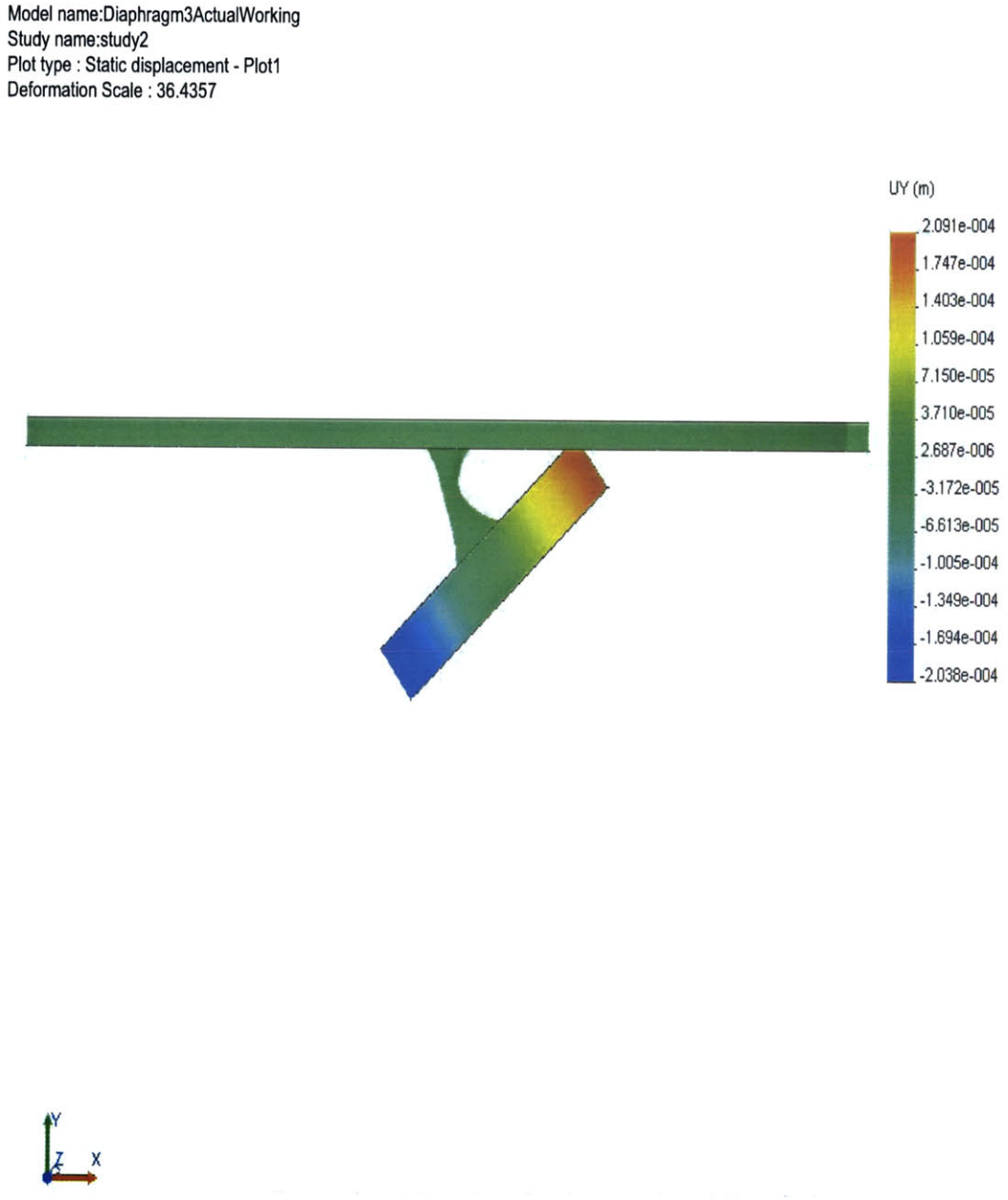

Figure 5-8: Pivot (Aluminum 7075) Displacement Study

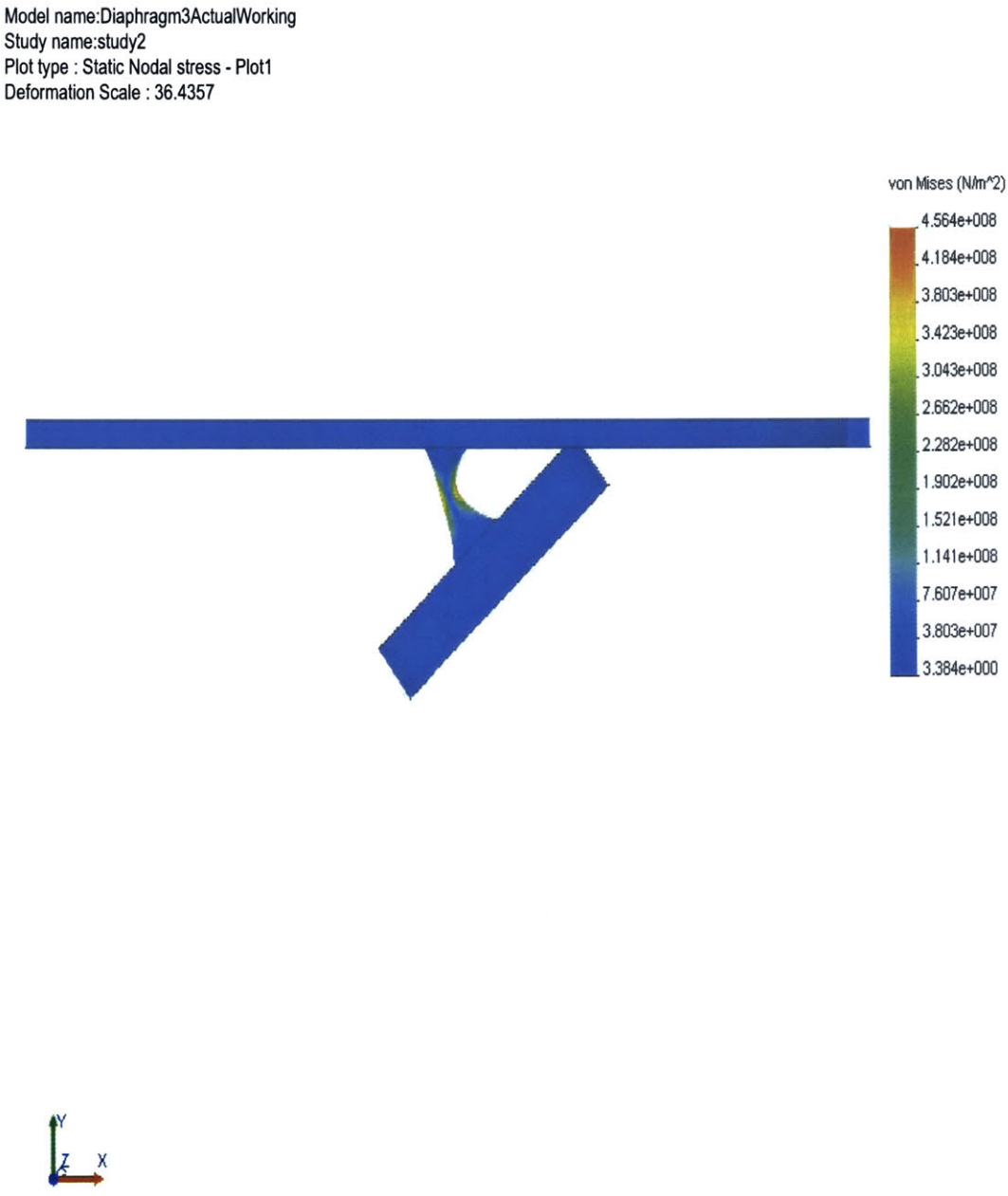

Figure 5-9: Pivot (Aluminum 7075) Stress Study

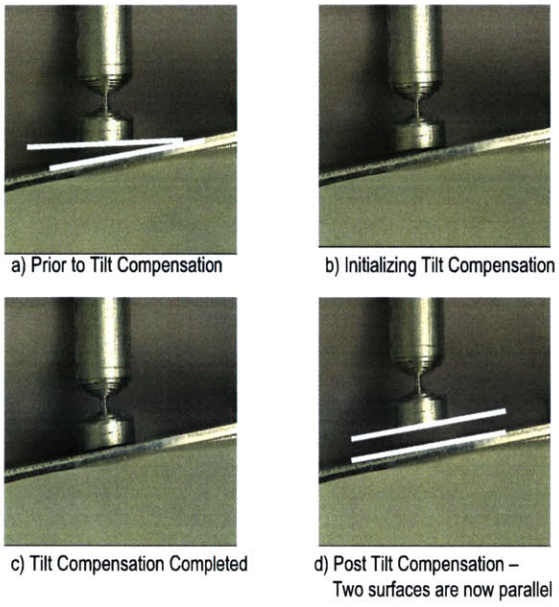

Figure 5-10: Demonstration of Tilt Compensation Flexure

variables used to design the prototype. The experiments showed that the valve can be controlled to a 1.8 nm positioning. Tilt compensation was visually verified.

Chapter 6

Conclusions and Recommendations

The design and experiments presented are a good first step towards achieving the desired user specifications and characterizing the design. More work, however, needs to be done to fully develop and test the design.

6.1 Short Term Recommendations

The closed loop response of the valve needs to characterized using the specified annular piezoelectric actuator. In addition, a second generation closed controller needs to be designed. The controller used for experiments presented in this thesis do not account for the hysteresis present in the system.

Preparations for a size exclusion test with the use of polystyrene latex spheres is underway and needs to be performed. Testing with biological samples can be done when the design receives the proper coating treatment.

Although a signal change was experimentally measured when a piezoelectric actuator hits an object on several occasions, the expected signal did not match predictions made by established models. The experiment and model need to be verified.

6.2 Long Term Recommendations

Because heat can distort the flat surfaces, all coatings must be cured at room temperature. This is a slow process. The search must continue for more desirable coatings.

A quantitative test for examining the degree of parallelism between the two flat surfaces needs to be developed. The design tilt compensation mechanism does work and can be measured down to the micron scale with a camera. Beyond the micron range, it will be difficult to measure.

6.3 Conclusion

This thesis sought to make contributions towards the development of a size based separation device for molecules in the size range of 0.5 nm to 500 nm. Design specifications were identified from the user standpoint and from an engineering standpoint. Gap positioning control of the proposed design has been shown to be controllable to at least 1.8 nm.

Bibliography

[1] *Techniques Used in Bioproduct Analysis.* Butterworth-Heinemann, 1992. Chapter 5, Written by R. Cannell.

[2] *ASME B46.1, Surface Texture(Surface Roughness, Waviness, and Lay).* ASME, 1995.

[3] *Machinery's Handbook.* Industrial Press, 26 edition, 2000.

[4] Nanopores for dna sequencing and single-molecule experiments. http://www.physics.brown.edu/Users/faculty/xsling/ling_group/nanopore.html, July 2003.

[5] Eray S. Aydil Alcantar, Norma A. and Jacob N. Israelachvili. Polyethylene glycol-coated biocompatible surfaces. *Journal of Biomedical Materials Research*, 51(3):343–351, September 2000.

[6] Karl F. Böhringer. Surface modification and modulation in microstructures: Controlling protein adsorption, monolayer desorption and micro-self-assembly. *Journal of Micromechanical Microengineering*, 13(4):S1–S10, July 2003.

[7] Joe Campbell. Where do voice-coil actuators fit in? http://www.machinedesign.com, August 2003.

[8] William C. Tang David Bame Chakraborty, Indrani and Tony K. Tang. Normally closed, piezoelectrically actuated microvalve. Technical report, NASA and Jet Propulsion Laboratory, January 2001. http://www.nasatech.com/Briefs/Jan01/NPO20782.html.

[9] Physik Instrumente Company. Spec sheet for p-306.10. http://www.physikinstrumente.de/pdf/P_305_306.pdf.

[10] Physik Instrumente Corporation. Pi basic designs tutorial. www.pi.ws, August 2003.

[11] Steven M. Cramer. Chromatography. http://www.rpi.edu/dept/chem-eng/Biotech-Environ/CHROMO/chromintro.html, March 2003.

[12] General Electric. The filtration spectrum. http://www.gewater.com/library/tp/710_The_Filtration.jsp, June 2003.

[13] Julie A. Last Dora K. Cheung Paul L. Gourley Follstaedt, Susan C. and Darryl Y. Sasaki. Protein adhesion on sam coated semiconductor wafers: Hydrophobic versus hydrophilic surfaces. Technical report, Sandia National Laboratories, December 2000. http://infoserve.sandia.gov/cgi-bin/techlib/access-control.pl/2000/003016.pdf.

[14] Robert A Freitas Jr. *Nanomedicine*, volume 1. Landes Bioscience, October 1999. http://www.foresight.org/Nanomedicine/.

[15] Matthew R. Bonen Jaime Ramirez-Vick Mariam Sadaka Garcia, Antonio A and Anil Vuppu. *Bioseparation Process Science.* Blackwell Science, 1999.

[16] Piezomechanik GmbH. Electronic supplies for piezomechanics: Amplifiers, pulsers, pc cards. http://www.piezomechanik.com – Catalogues Link. Brochure.

[17] Peter Griffith and Alex Marien. Optical fabrication relies on tried and true methods. *Laser Focus World*, October 1997.

[18] Charles Heidi. Silicone rubber for medical device applications. www.devicelink.com/mddi/archive/99/11/003.html, February 2004.

[19] Belal M. Helal. Uv imaging of electrophoresis gels: a non-invasive nanogram level quantification of dna. Master's thesis, Massachusetts Institute of Technology, 77 Massachusetts Avenue Cambridge, MA 02139, February 2002.

[20] Schmitt MEasurement Systems Inc. Roughness average, ra. http://www.schmitt-ind.com/pdf/Roughness.pdf, August 2003.

[21] Jacob Israelachvili. http://squid.ucsb.edu/ sfalab/mark-II.html, January 2003.

[22] L. James Lee Liyong Yu Kurt W. Koelling Lai, Siyi and Marc J. Madou. Micro- and nano-fabricaiton of polymer based microfluidic platforms for biomems applications. In Luke P. Lee Manginell, Ronald P. Jeffrey T. Borenstein and Peter J. Hesketh, editors, *BioMEMS and Bionanotechnology*, volume 729, pages 17–27. Materials Research Society, Materials Research Society, 2002.

[23] Jim Lipman. Microfluidics puts big labs on small chips. *EDN*, 44(26):79–86, December 1999. http://www.e-insite.net/ednmag/contents/images/46419.pdf.

[24] Hong Ma. Instrumentation for the nanogate. http://www.media.mit.edu/resenv/nanogate/, January 2003.

[25] Carl R. Nave. Hyperphysics website. http://hyperphysics.phy-astr.gsu.edu/hbase/hframe.html, January 2003.

[26] University of Iowa College of Public Health. Fact sheet: Acrylamide. http://www.public-health.uiowa.edu/baecps/factsheets/Acrylamide.pdf, July 2003.

[27] Hong Kong University of Science and Technology. The hazards of electrophoresis. http://www.ab.ust.hk/sepo/tips/ls/ls008.htm.

[28] Edmnund Industry Optics. Using optical flats. http://www.edmundoptics.com/techSupport/DisplayArticle.cfm?articleid=254, June 2004.

[29] Andre Bernard David Juncker Niels B Larsen Bruno Michel Papra, Alexander and Emmanuel Delamarche. Microfluidic networks made of poly(dimethylsiloxane), si, and au coated with polyethylene glycol for patterning proteins onto surfaces. *Langmuir*, 17(13):4090–1095, June 2001.

[30] J.M. Paros and L. Weisbord. How to design flexure hinges. *Machine Design*, pages 151–156, November 1965.

[31] Miguel Perez III. Capillary electrophoresis. http://ntri.tamuk.edu/ce/ce.html, March 2003.

[32] PiezomechanikPiezo. Piezo-mechanical and electrostrictive stack and ring actuators: Product range and technical data. www.piezomechanik.com – Catalogues Link. Brochure.

[33] Walter D. Pilkey. *Formulas for Stress, Strain, and Structural Matrices.* Wiley Interscience, 1994.

[34] Manzoor Shah. Ultra mechanotronic filtration (ultramf): Looking into the distant future. email, November 2002.

[35] Ketul C. Popat Sharma, Sadhana and Tejal A. Desai. Controlling nonspecific protein interactions in silicon biomicrosystems with nanostructured poly(ethylene glycol) films. *Langmuir*, 18(23):8728–8731, November 12 2002.

[36] Alex Slocum. Design of three-groove kinematic couplings. *Precision Engineering*, 14(2):67–76, April 1992.

[37] Byron Stancil. Design of a programmable filter for macromolecules. Master's thesis, Massachusetts Institute of Technology, 77 Massachusetts Avenue Cambridge,MA 02139, June 2002.

[38] ADE Technologies. Non-contact capacitance gauging instrument brochure. http://www.adetech.com/pdf/4810withprobesreve.pdf, June 2004.

[39] Unknown. Gel electrophoresis. http://www.bergen.org/AAST/Projects/Gel/, March 2003.

[40] Joseph Fu Vorburger, Theodore and Ndubusi Orji. In the rough. *OE Magazine*, 2(3):31–34, March 2002.

[41] Stefan Vorndran. Why nanopositioning is more than just nanomters - or how to find a state-of-the-art-system. http://www.nanopositioners.com/State-of-the-Art-NanoPositioningSystemsPI.pdf, July 2003.

[42] Karl Voss. Dna analysis by capillary electrophoresis. http://hobbes.chem.ualberta.ca/ karl/titlepg.html, March 2003.

[43] Matrin Hegner Hans-Joachim Gutherodt Wagner, Peter and Giorgio Semenza. Formation and in situ modification of monolayers chemisorbed on ultraflat template-stripped gold surfaces. *Langmuir*, 11(10):3867–3875, October 1995.

[44] Richard F. Wallin. Biocompatibility guidelines, using eto with parylene. *Medical Device & Diagnostic Industry Magazine*, page 82, January 1998. www.devicelink.com/mddi/archive/98/01/017.html.

[45] Baishi Wang. Nanotopography of silicon wafers:using the chapman non-contact profiling system. http://www.chapinst.com/applicationnotes/nanotopography.pdf, June 2004.

[46] Hui Wang and Daniel Branton. Nanopores with a spark for single-molecule detection. *Nature:Biotechnology*, 19(7):622–623, July 2001. http://www.nature.com/cgi-taf/DynaPage.taf?file=/nbt/journal/v19/n7/full/nbt0701_622.html.

[47] James White. *The Nanogate:Nanoscale Flow Control.* PhD thesis, Massachusetts Institute of Technology, 77 Massachusetts Avenue Cambridge,MA 02139, May 2003.

[48] Shon W. Yim. *Dynamics of Sliding Mechanisms in Nanoscale Friction.* PhD thesis, Massachusetts Institute of Technology, 77 Massachusetts Avenue Cambridge, MA 02139, June 2002.

[49] Kevin Yip. Chromatography. http://www.rpi.edu/dept/chem-eng/Biotech-Environ/IONEX/be_intro.htm, June 2004.

[50] Tejal Desai Zhang, Miqin and Mauro Ferrari. Proteins and cells on peg immobilized silicon surfaces. *Biomaterials*, 19(10):953–960, May 1998.

Appendix A

Disregarded Design Ideas

A.1 Appendix A Summary

This section presents other design ideas that were conceived with as much detail as possible. Design commentary is presented to demonstrate why these designs were not chosen.

A.2 Design 1 – Tubular Filtration

A.2.1 Material Selection

The material chosen for the flat plates for this design was Fused Silica [37]; it was purchased from the Valley Design Corporation. Fused Silica has extremely low thermal expansion; the coefficient of thermal expansion is equal to 0.55 x 10^{-6} per °C. Dimensions of the plates are 5 mm x 13.5 mm x 5 mm. At this dimensional scale roughness, waviness, and flatness all contribute to the minimum gap size that can be created. Roughness of the material can be decreased to less than 5 Angstroms. Waviness and flatness wavelength are difficult to separate at this scale. The amplitude of the asperities, however, can still be described as 1/10 wave, meaning that the distance from the highest peak to lowest valley is approximately 50 nm on the surface of each plate. Aquarium silicone was selected as the sealant surrounding the flat plates for it's elastic, waterproof nature, and sealing properties [37]. Silicone and polypropylene tubing was selected as the outer material for it's flexibility, inert characteristics, and low cost.

A.2.2 Manufacturing Process

The Fused Silica plates were manufactured by lapping and polishing. A conventional milling machine was used to manufacture the plate holders. A second adhesive/sealant and two .07 inch screws were used to secure the flat plates inside the flat plate holders. Square apertures just large enough for the plate holders were cut out of the tubing. The plate holders and plates were placed so that the Fused Silica surfaces touch. Once in place, an injection needle filled with aquarium silicone filled and sealed the gaps. The aquarium sealant was viscous enough to fill the gaps. The filtering element was thus completed.

A.2.3 Design Commentary

Of the possible choices for flat plates (borosilicate glass, fused silica, quartz, and silicon, zerodur), fused silica is a legitimate choice. Its coefficient of thermal expansion is extremely low (only zerodur can be better with 0.15 x 10^{-6} per °C) when the temperature is between 0 and 50 °C. Flatness can be improved to 1/20 of a wave (25 nm peak to valley on each plate) using the lapping/polishing method. Flatness better than 1/20 of a wave is possible but extremely expensive. Using silicon coated with a layer of titanium and gold molded by a mica would improve roughness to about 1 angstrom, and waviness to about 1 - 2 nm. Flatness may also improve with this method, but needs to be evaluated experimentally.

One major benefit to the design is that the flat sections will not deform when the gap increases in size. As a result of holding the plates in the aluminum holders, the flat plates will be less prone to failure by hysteresis and fracture. In addition, the dimensional scale of the plates has the added benefit that stiction is less of an issue because elastic forces dominate at this scale. Stiction typically becomes an issue when dimensions cross below 1 mm [6]. Observations of the motion of a simple model showed that one actuator can not be used to control the gap size (See Figure A-1 for a diagram of how the pieces deform with one and two actuators). Two actuators improve the alignment, but still may not be good enough for this application. Additionally, the elastic material mechanical properties (Force-strain relationship, elongation limit, etc.) must be well understood in order to gain control of the gap size. This analysis is rather complex but good results can be achieved through Finite Element Analysis(FEA). It so happens that elastomers are not linearly elastic for

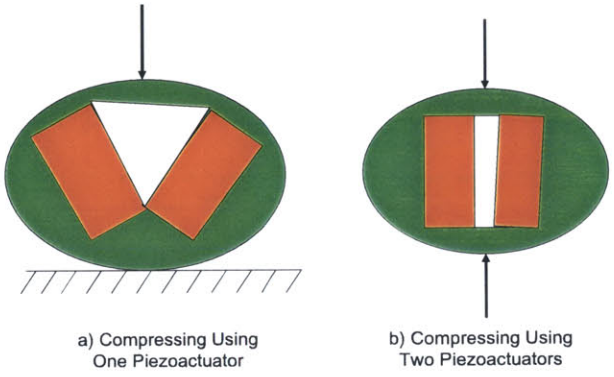

Figure A-1: Displacement With Applied Force

large deformations. It is unclear at this point whether displacements at the nanometer level are also non-linear. Stiffness needs to be precise.

The fluid flow system on this dimensional scale is not adequate. A quick approximation proves the point. Making the assumption that a perfect minimum sized gap of 0.5 nm can be created and recalling the Poiseuille flow equation: $Q = \frac{Wh^3}{12\mu_{viscosity}} * \frac{dP}{dx}$ (See Chapter 3). In this case we desire Q = 10 μL/min. The dimensions of the gap are w = 13.5 mm, h = 5 nm dx = 5 mm (See Figure A-2). Assuming water is the fluid μ = 0.001 Ns/m^2. The change in pressure(dP) is then approximately 5900 GPa. This seems unrealistically high. The pressure could be lowered by making the flat plates thinner and wider. This may not be a good option when considering the consequences of inadequate surface flatness of a wider plate and reduced structural strength of a thinner plate.

A.2.4 Design 1 – Bottom Line

The design as it stands is not acceptable. If this filtering element worked perfectly on the mm size scale, particle separation in the 0.5 nm - 50 nm range might not be adequate. This limitation could possibly be reduced to 20 - 30 nm with better flatness but with great

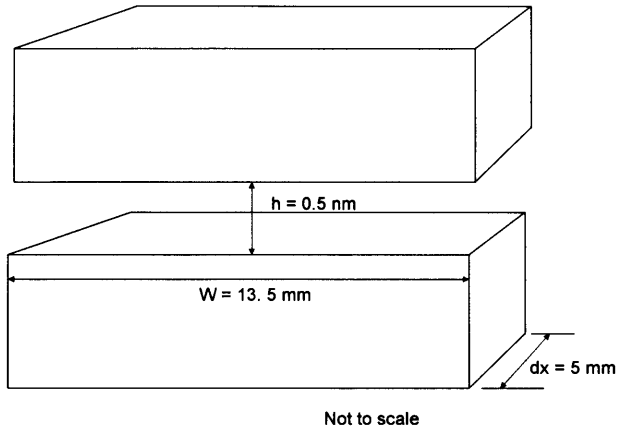

Figure A-2: Tubular Filtration - Gap Drawing

expense. The flow rate for this design is also not acceptable. The use of a polymer sealant may also not be the best choice for the surrounding material. Although it is an excellent sealant, the thermal stability of polymers is not as good as for metals. Metals, however, are not good sealants. With regards to manufacturing of this device, it is too complex. Using a needle to insert the silicone sealant is not well controlled, the end product looks messy. A better option might be to manufacture the entire section that surrounds the flat plates by means of a mold (See Figure A-3).

Miniaturization and multiplication of this design may be an option. Brainstorming sessions to this point, however, have revealed that it may be too complex. Among other things, miniaturization requires that one figure out how to integrate polymers into the fabrication process. Current manufacturing methods destroy polymers because of the high temperatures required in the manufacturing processes.

The good lessons to learn from this design are worth noting. The fact that the flat plates do not deform when moving is desirable. Also, the surface profile of this design can be examined (this is very important, if it can be examined and measured it can be improved). In addition to the surface profile, it would be relatively easy to add a coating

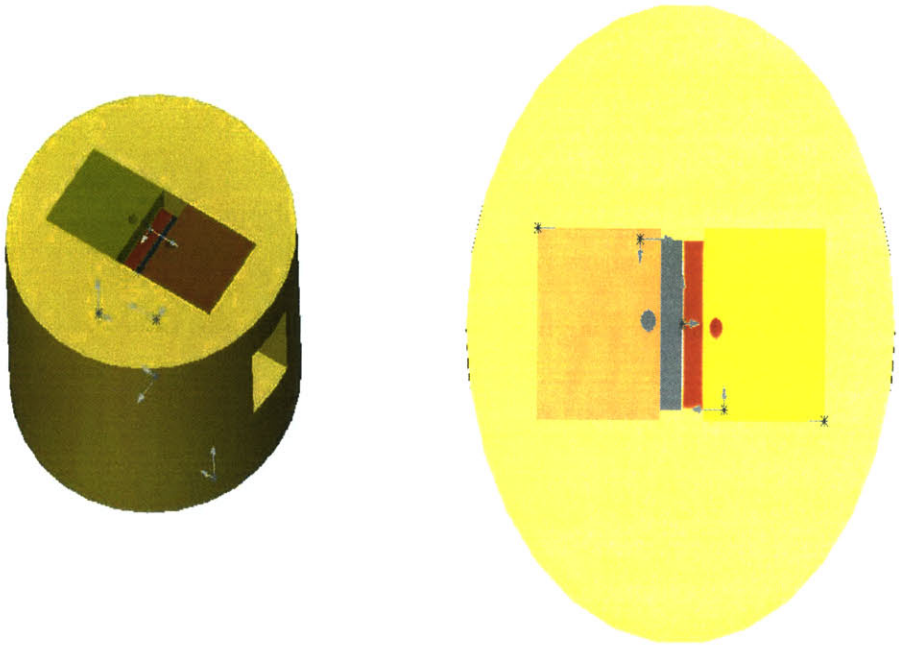

Figure A-3: Tubular Filtration - Molded Tube Version

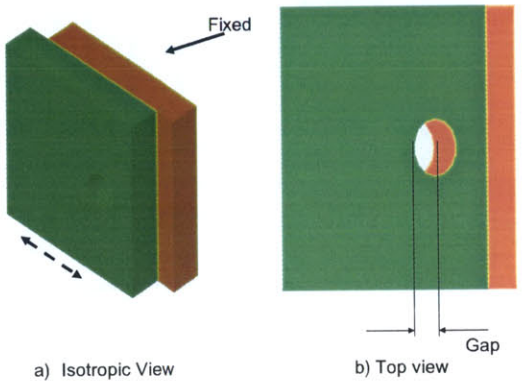

Figure A-4: Substrate Sliding

to the surfaces coming in contact with the fluid to be filtered.

A.3 Design 2 - Sliding Substrates

A.3.1 Overall Design Description

The concept of this design is to place two flat plates with etched holes on top of each other. One of the flat plates is to be held fixed, while the other is to slide on the bottom plate. Alignment or mismatch of the holes is used to create the gap (See Figure A-4).

A.3.2 Material Selection

The substrates would either be a glass/ceramic or silicon.

A.3.3 Manufacturing

Manufacturing of the substrates would be relatively simple. All it would involve is etching and thin film deposition. Hole sizes could be 500 nm or greater which is easily achieved by conventional microfabrication techniques. Coating of the holes may be practically difficult.

A.3.4 Design Commentary

In order for this concept to satisfy the user-requirements, the plate sliding must be controllable at angstrom increments. An understanding of the physics associated with the sliding surfaces is thus essential. This proves extremely challenging.

Friction and wear are terms that are often used to describe the physics of a body sliding on top of a surface. Friction is defined as the resistive force to the sliding of the body in motion. Wear is defined as the removal of material of one or both of the contacting surfaces.

The classical (DaVinci and Amonton) explanation for friction stated that when two surfaces came in contact the high points of microscopic asperities plastically deformed until they could support the applied load. These deformed asperities bonded. Friction as a result became understood as the force required to break these bonds. As a result of this theory the motion of a sliding object was thought to be the continual breaking and forming of asperity deformations. This breaking and forming caused wear. One would theorize that by reducing the amount of attraction of the interaction between the surfaces would reduce the friction. This may be inconsistent because there is no evidence that a correlation between the force to separate the two objects is correlated to the resistance to lateral motion.

This classical theory of friction is not applicable to MEMS devices. Surface roughnesses tend to be low for MEMS based materials (nanometer or better) which reduces the likelihood of plastic deformation. In addition, MEMS designs tend to be so thin that there may not be enough dislocations in the material to allow for plastic deformation. As a result, friction may occur without much wear – interatomic models might be more appropriate to describe the sliding motion [48].

In addition to the problem of friction is wear. If wear occurs as a result of the sliding motion the surfaces will be effectively destroyed. Gaps between the surfaces or the failure of one or both pieces may result.

A.3.5 Design 2 – Bottom Line

A major advance in the understanding and control of friction needs to be accomplished for this idea to work. The reason for the increased concern for friction as devices get smaller beyond the microscale is that the relevant forces are not the same as in the macroscale. As

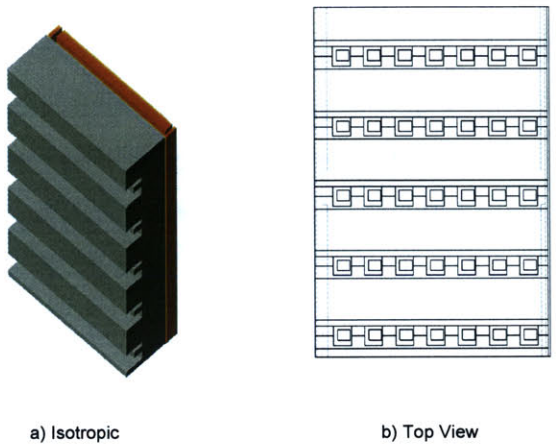

Figure A-5: Flexure Idea 1

objects shrink the surface area to volume ratio decreases increases – surface forces become dominant over the inertial forces. These surface forces are not yet clearly understood.

The main advantage of this design is that different shapes could potentially be etched on the two surfaces. Adding the different shapes could add to the differentiation between two molecules.

A.4 Design 3 – Flexure Based Design

A.4.1 Overall Design Description

This concept is inspired by Design 2. It consists of two plates. The bottom plate would contain extrusions while the top plate would include holes. The extrusions would fit into the holes and the mismatch between extrusions and holes would be used as the gap (See Figure A-5). The bottom plate would be held fixed, while the top portion of the design would be allowed to move by deformation of bonded portions of top and base plate.

A.4.2 Material Selection

Silicon would be chosen because most fabrication techniques are optimized for it. Additionally, a PEG coating would have to be applied.

A.4.3 Manufacturing

The idea can be manufactured by microfabrication techniques. Holes can be etched to desired size (500 nm across because that is the largest molecule to allow through).

A.4.4 Design Commentary

It is theoretically possible to create the desired a gap of 0.5 nm dimension. This depends on the ability to create a surface with adequate roughness and the degree of motion control. It is not so clear that adequate roughness is possible with available manufacturing methods. Roughness is dependent on the size of the desired hole, thickness of the plate, and the etch rate. A slower etch rate produces a more favorable roughness.

The motion concept portion of this design is favorable. Only one actuator and one sensor are needed to regulate the gap. There will be difficulty, however, in actuation devoid of top plate buckling. In addition, holding the bottom plate fixed is crucial. Any wavering of the bottom plate would significantly impede a controlled motion.

It is clear that thickness of the plates has an important role in this design. Thickness is dependent on two factors: its ability to move without buckling (sustain mechanical forces) and the limitations of techniques that can create the holes of the top plate. The factors do not necessarily complement each other. In fact, they may be in opposition to each other.

A.4.5 Design 3 – Bottom Line

Motion control in combination with multiple filtering elements are the most desirable aspects of this design. With one actuator and one sensor, multiple filtering elements can be controlled.

This design is not adequate because of flow control. There is little room for error in the manufacturing because of many places where a leak could form. In addition, the collection

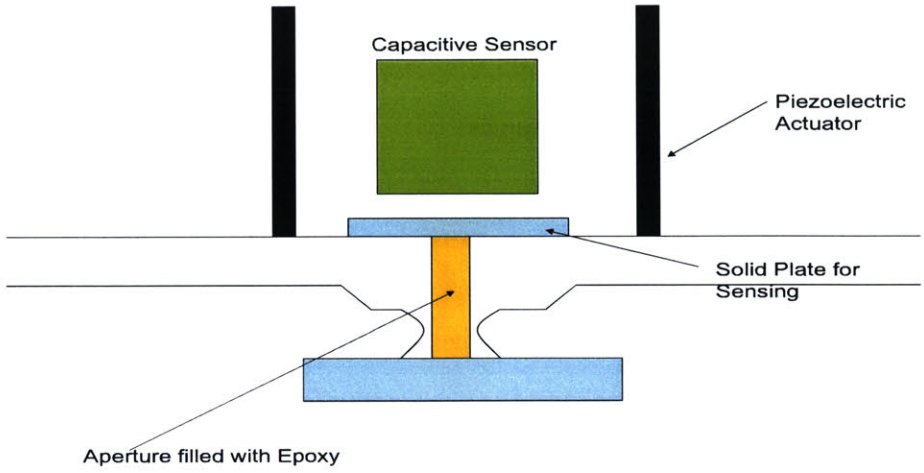

Figure A-6: Close-up cross-section of diaphragm with pivot

of the filtered molecules is too disordered.

A.5 Considered Pivot Designs

The mechanism is to be compliant prior to conforming to the base plate. After mating and tilt-compensation has been applied it is expected that the pivot become maintain the deformed shape and become stiffer. Several options were investigated towards achieving this goal. Ideas ranged from using eletrorheological fluids (or solids)to re-designing the pivot with shape memory alloy based self-locking mechanisms. In the end it was decided that a pivot could be manufactured and stiffened by the addition of an epoxy. The epoxy could be placed around the pivot or a hole could be cut through the center of the diaphragm to provide an inlet. The latter option was chosen because it is cleaner, provides better accessibility and allows more robust options for the epoxy. With this design, the epoxy need not be biologically compatible because it does not come in contact with the fluids to be separated. The epoxy will not provide a good surface for the capacitive sensor to work with. As a result, a cover must be placed on top of the epoxy.

Appendix B

Calibration of The Capacitance Probes

Calibration of the capacitance probe is typically done by the manufacturer through the use of a laser interferometer. The calibration can be coarsely checked with a holder for the probe, a sensing target, and a stage micrometer (For the set up Please see Figure B-1). The probes used in experiments for this research were checked according to this method. The stage micrometer was able to position the target to within 10 microns.

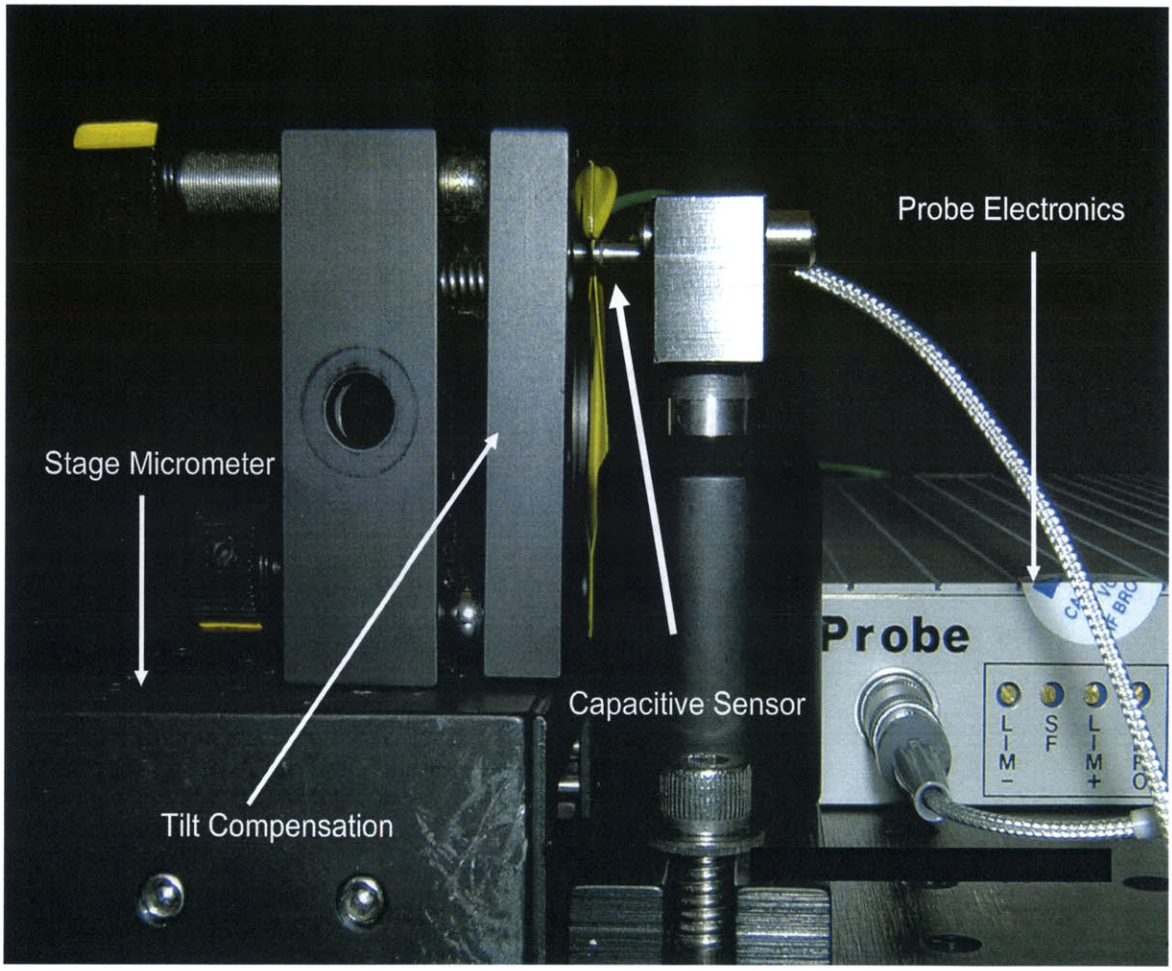

Figure B-1: Capacitance Probe Calibration Check

Appendix C

Specification Sheets of Purchased and Used Equipment

This appendix provides the spec sheets for the equipment used and purchased for this thesis.

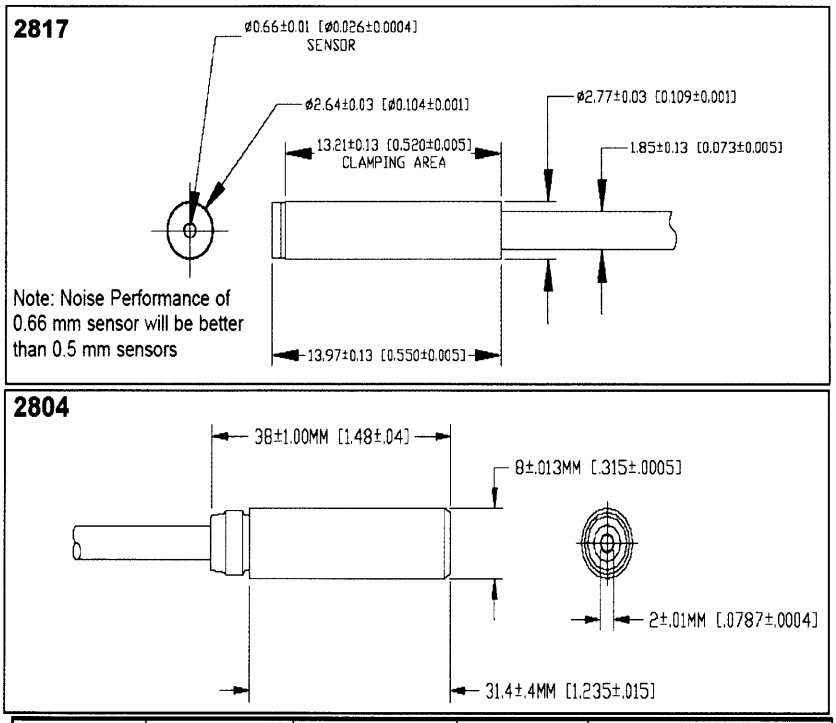

PROBE	Standoff	Range	Resolution	Analog Output
2817	10 microns	+/- 10 microns	0.10 nm	+/- 10 Volts
2804	100 microns	+/- 50 microns	0.5 nm	+/- 10 Volts

Figure C-1: Specifications for Used Capacitance Probes
These probes were used for testing of the apparatus. Pictures courtesy of ADE Technologies [38]

Analog Amplifiers SVR

Low voltage/high voltage types available
Lowest noise levels
Semibipolar operation
for enhanced actuator stroke/force generation

SVR 150/1 (single channel)
SVR 150/3 (3 independent channels)

Voltage range:
–30 V thru +150 V (semibipolar)

Manual setting of DC-Offset
(superimposed to external signal)

Variable attenuation

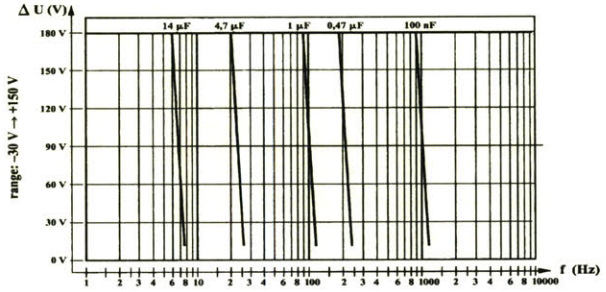

Input:

Signal:	+/–5 V (+/–10 V with attenuation)
Impedance:	5 kOhms
Connector:	BNC

Output:

Connector:	BNC
Voltage total:	–30 V thru +150 V
DC-Offset range:	–30 V thru +150 V
Gain:	30 (without attenuation)
Max. current:	60 mA
Noise:	0.3 mVpp (for 4.7 µFarad load)
Display:	LCD
Dimensions W x D x H (mm):	
single channel:	165 x 200 x 65
3-channels:	260 x 320 x 155
Weight (kgs):	
single channel:	1.75
3-channels:	4.7

Additional features of 3 channel SVR 150/3 amplifier:

Monitor BNC output per channel:
shows 1:1000 piezo voltage
LC-Display per channel

Option:

Parallel or serial interface (12 bit resolution)

On request:

Amplifiers SVR 200 for voltage range
–50 V thru +200 V/40 mA

12

Figure C-2: Specifications for Piezoelectric Amplifier used in Chapter 5 experiments This amplifier was used in experiments using Pictures courtesy of Piezomechanik [16]

A 2

PSt 150/7/... VS12

General data: see brochure: "Piezomechanics: An Introduction"
Prestress force = max. tensile force = 300 N
Max. load force: 1800 N
Max. force generation: 1800 N
Open loop sensitivity at 1 mV noise for actuator PSt 150/7/7: 0.05 Nanometer

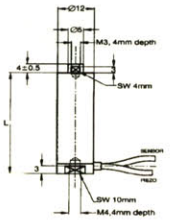

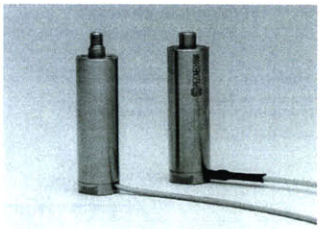

Type	max. stroke µm	length L mm	el. capacitance µF	stiffness N/µm	resonance frequency kHz
PSt 150/7/7 VS12	13/9	19	0.7	120	40
PSt 150/7/20 VS12	27/20	28	1.8	60	30
PSt 150/7/40 VS12	55/40	46	3.6	25	20
PSt 150/7/60 VS12	80/60	64	5.4	15	15
PSt 150/7/80 VS12	105/80	82	7.2	12	12
PSt 150/7/100 VS12	130/100	100	9	10	10
PSt 150/7/120 VS12	160/120	118	11	8	8
PSt 150/7/140 VS12	190/140	136	13	7	6
PSt 150/7/160 VS12	210/160	154	15	6	5

Standard configuration:

Tapped hole in moving end
Electrical connection: 1 m coaxial cable RG 178 with BNC connector

Options:

Coaxial cable RG178 with LEMOSA connectors 00250 or 0S250

Moving end with spherical endpiece **VbS**
Moving end with threaded pin **VAg**
Moving end plane **pF**
Thermostable modification
Low temperature modification
UHV compatibility
Position detection

Accessories see section C

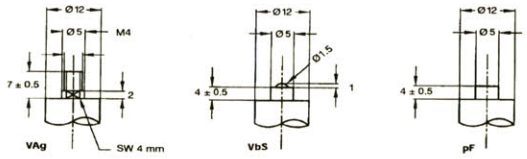

11

Figure C-3: Piezoelectric used in Chapter 5 experiments
Probe number PSt 150/7/20 VS12 was used. Pictures courtesy of Piezomechanik [32]

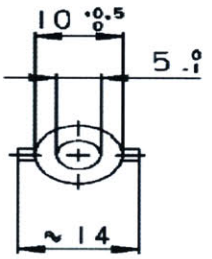

P-305 dimensions (in mm)

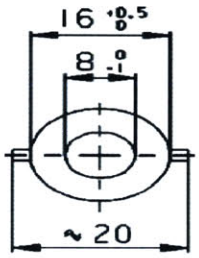

P-306 dimensions (in mm)

Technical Data

Models	P-305.00	P-305.10	P-305.20	P-305.40	P-306.00	P-306.10	P-306.20	P-306.40	Units	Notes see p. 1-41
Open-loop travel @ 0 to −1000 V	5	10	20	40	5	10	20	40	µm ±20%	A4
* Open-loop resolution <	0.05	0.1	0.2	0.4	0.05	0.1	0.2	0.4	nm	C2
**Static large-signal stiffness	182	121	70	37	469	313	179	94	N/µm ±20%	D1
Push/pull force capacity	500 / 20	500 / 20	500 / 20	500 / 20	800 / 40	800 / 40	800 / 40	800 / 40	N	D3
Max. operating voltage	-1000	-1000	-1000	-1000	-1000	-1000	-1000	-1000	V	A7
Electrical capacitance	25	40	65	120	55	90	180	350	nF ±20%	F1
Dynamic operating current coefficient (DOCC)	6.25	6.25	6.25	6.25	14	14	14	14	µA/(Hz x µm)	F2
Unloaded resonant frequency (f_0)	20	14	12	8	10	8.5	7	5.5	kHz ±20%	G2
Standard operating temperature range	-20 to 80	-20 to +80	-20 to +80	-20 to +80	-20 to +80	-20 to +80	-20 to +80	-20 to +80	°C	
Wire leads	PTFE, 100 mm ±5 mm, Ø 1.3	PTFE, 100 mm ±5 mm, Ø 1.3	PTFE, 100 mm ±5 mm, Ø 1.3	PTFE, 100 mm ±5 mm, Ø 1.3	PTFE, 100 mm ±5 mm, Ø 1.3	PTFE, 100 mm ±5 mm, Ø 1.3	PTFE, 100 mm ±5 mm, Ø 1.3	PTFE, 100 mm ±5 mm, Ø 1.3		
Weight	4.3	6.3	10.3	20.5	9.5	17	24.2	46	g ±5%	K
Length	8	12	21	40	8	12	21	40	mm ±1	
Recommended Amplifier (codes explained p. 6-46)	B, I	B, I	B, I	B, I	B, I	B, I	B, I	B, I		

** Resolution of PZT actuators is not limited by friction or stiction. Noise equivalent motion with E-507 amplifier*
*** Dynamic small-signal stiffness -50% higher*

Figure C-4: Piezoelectric Actuator specified in Chapter 4
Pictures courtesy of Physik Instrumente [9]

Technical Data

Models	E-461.00
Function	Power amplifier
Channels	1
Maximum output power	0.5 W
Average output power	0.3 W
Peak output current < 5 ms	0.5 mA
Average output current > 5 ms	0.3 mA
Current limitation	Short-circuit proof
Voltage gain	-100 ±1
Polarity	negative
Control input voltage	0 to +10 V
Output voltage	-10 to -1000 V
DC-offset setting	-10 to -1000 V at output with 1-turn pot.
Input impedance	10 kΩ
Frequency response	Static and quasi static applications only
Control input socket	BNC (E-461.00 only)
PZT voltage output socket	LEMO ERA.0A.250.CTL
Dimensions	160 x 90 x 60 mm
Weight	0.5 kg
Operating voltage	10 to 15 VDC, stabilized
Max. operating current	80 mA
Operating temperature range	0 to +60°C
Power supply	Not included (3.5 mm jack socket)

Figure C-5: Piezoelectric Actuator specified in Chapter 4
Pictures courtesy of Physik Instrumente [9]

Appendix D

Drawings and Pictures of the Machine

This section contains selected drawings and pictures for the parts manufactured.

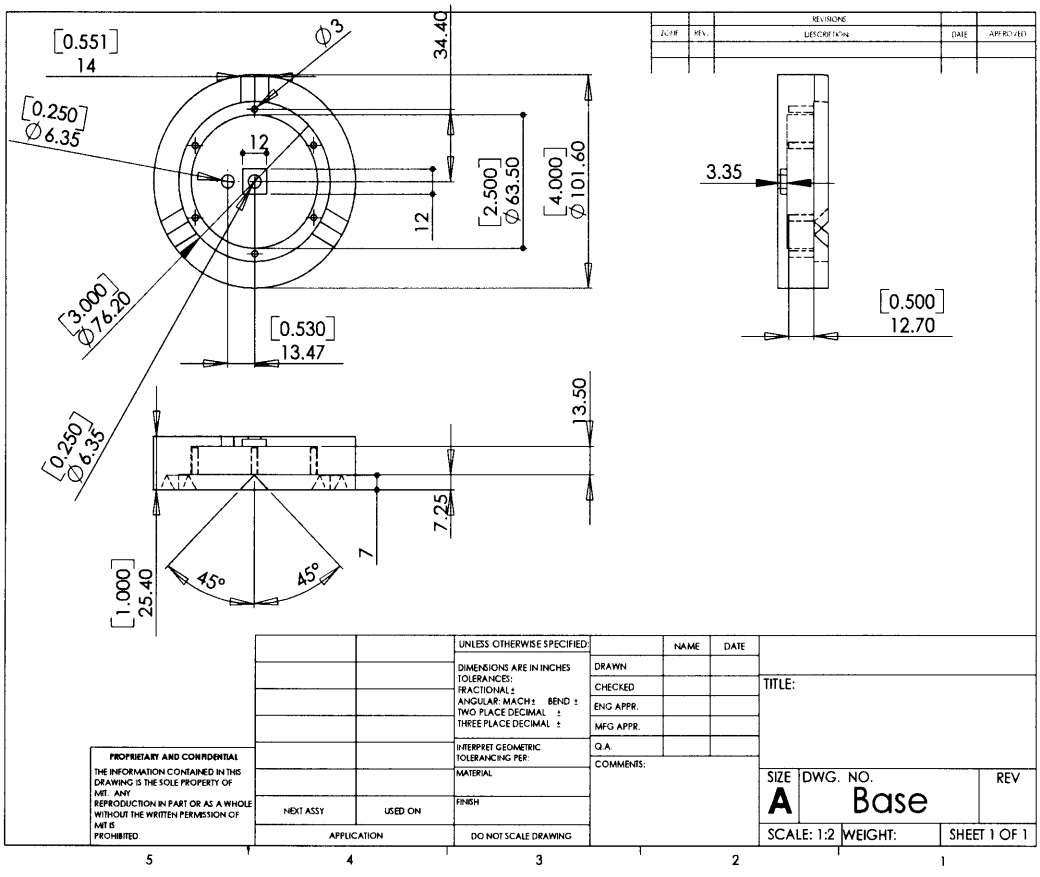

Figure D-1: Base Specs

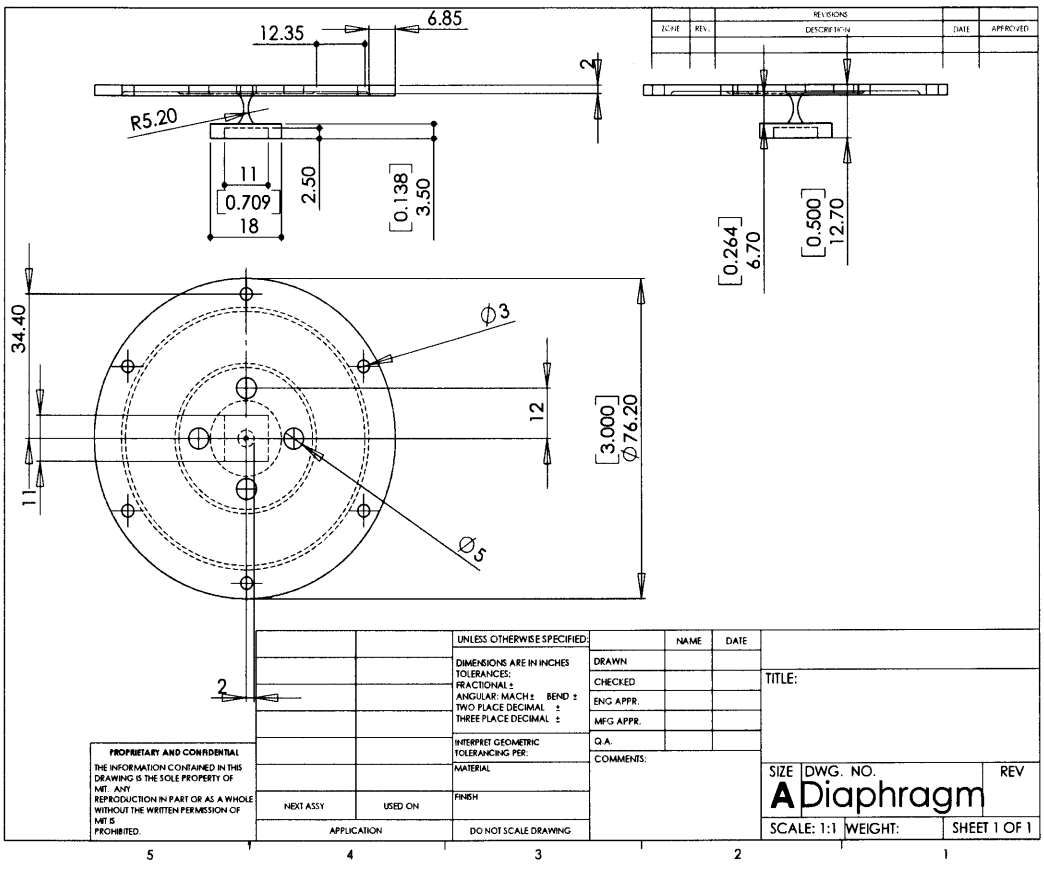

Figure D-2: Diaphragm Specs

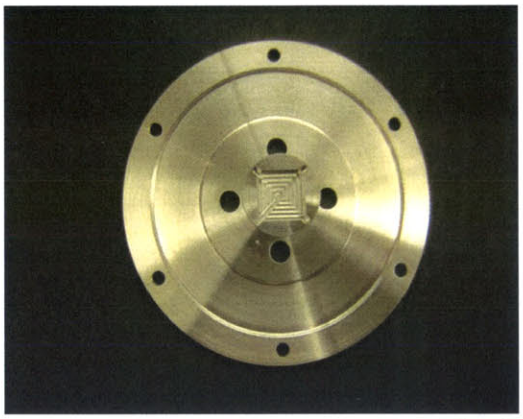

Diaphragm (bottom side)

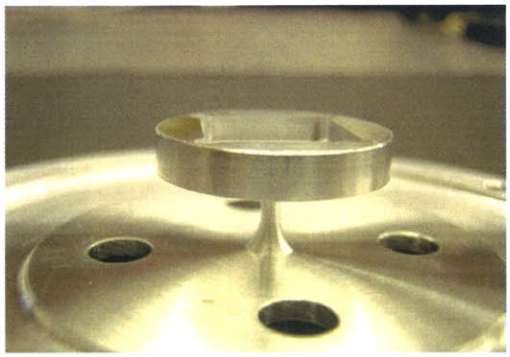

Close up of Pivot

Figure D-3: Built Diaphragm Pictures